



Faculty of Biosciences, Fisheries, and Economics, Department of Arctic and Marine Biology

Metabolomic and metagenomic study of Lake Baikal diseased sponges

Are toxic cyanobacteria to blame?

Yelena Churakova

Master's thesis in Molecular Environmental Biology BIO-3950 August 2020



Table of Contents

1	Introduction	1
1.1	The Largest Freshwater Lake in the World.....	1
1.2	The Sponge Holobiont	2
1.3	Cyanobacteria and Their Natural Products	4
1.4	Sponge Disease History, Globally and Locally	6
1.5	Thesis Aims.....	9
2	Materials and Methods	10
2.1	Specimen Procurement.....	10
2.2	Extraction of Secondary Metabolites from Sponge and Biofilm Specimens.....	12
2.2.1	Aqueous Extraction	13
2.2.2	Organic Extraction	13
2.2.3	Mass Spectrometry Sample Preparation	14
2.3	Mass Spectrometry	14
2.4	Metagenomic Analysis	15
2.5	Statistical Analysis	16
	Results.....	17
2.6	UHPLC-HR-MS/MS Metabolic Profiling	17
2.6.1	Healthy Sponge Comparative Chromatograms.....	17
2.6.2	Healthy Versus Unhealthy Sponge Chromatograms.....	20
2.6.3	Search for Identifiable Molecules	24
2.6.4	Global Natural Product Social Molecular Networking (GNPS)	26
2.7	Sponge-Associated Microbial Communities.....	27
2.7.1	Differences in Phyla	27
2.7.2	Differences in Cyanobacterial Communities	28
2.7.3	Differences in Proteobacteria and Bacteroidetes Communities	31
2.7.4	Dissimilarities at Phylum Level	32

3	Discussion	34
3.1	Specimen Diversity	34
3.2	Metabolic Profiling	34
3.2.1	Mass Spectrometry Chromatograms	34
3.2.2	Search for Cyanobacterial Natural Products	36
3.2.3	Global Natural Product Social Molecular Networking	36
3.2.4	Untargeted Metabolomics Limitations	38
3.3	Metagenomic Profiling	39
3.3.1	Changes in Microbial Community Structure	39
3.3.2	Decrease in Symbiont Cyanobacteria	39
3.3.3	Similar Trends in Proteobacteria and Bacteroidetes Phyla	40
3.3.4	Non-microbial Disease Etiology	41
4	Conclusion and Outlook	42
5	References	43
	Appendix	53
	Appendix 1	53
	Appendix 2	56
	Appendix 3	58
	Appendix 4	60

List of Tables

Table 1: Operating conditions of the VION IMS QToF Mass Spectrometer.	15
Table 2: The relative peak intensities (%) of the molecules annotated in Figure 6, displaying similarities and differences between the metabolic output of healthy sponge specimens of different genera.	19
Table 3: The relative peak intensities (%) of five molecules identified by their probable chemical structures, based on their similar retention times (RT), mass-to-charge ratios (m/z (H+)), and fragmentation patterns, found in the healthy and unhealthy sponge specimens. Dashed lines indicate that the compound was not detected at the minimum of 30,000 detection units used to filter the molecules.	26
Table 4: Details about the specimens received for this study including specimen ID, sampling location, and observational and microscopy-aided descriptions of healthy and diseased sponges and biofilms. Images of most specimens in the lab, taken after collection and before lyophilization, are also included. The image for L_H1 was taken during collection and the image for R_U1 is not available.	53

List of Figures

Figure 1: The approximate location and size of Lake Baikal within Siberia, Russia, which is surrounded by a black box. Figure retrieved from Khanaev et al., 2017.	1
Figure 2: Image of the three types of sponge structures with some labelled parts of the body. Arrows indicate the flow of water through the chambers of the different structures. Demosponges generally have the most complex body structure (leuconoid). Figure retrieved from Hogg et al., 2010.	3
Figure 3: A map of Lake Baikal with the three specimen sites marked in the map insert in the top left corner. Sponges were collected from the littoral zone of the lake associated with the marked sites. The map was modified from Khanaev et al., 2017.	10
Figure 4: Images from the scuba diving session for specimen collection. A healthy <i>Lubomirskia baikalensis</i> sponge is pictured in (a), an unhealthy bleached <i>Lubomirskia baikalensis</i> sponge is pictured in (b), and an unhealthy <i>Baikalospongia</i> sp. with an attached dark purple biofilm is pictured in (c). Images courtesy of Irina Tikhonova.	11
Figure 5: a) An overview of the specimens from four different genera in the <i>Lubomirskiidae</i> family of endemic Lake Baikal sponges and biofilm specimens unassociated with sponges. b)	

A simplified workflow of the process to extract mass spectrometry data from sponge and biofilm specimens. The steps for the organic extraction are labelled from (1) grinding down the lyophilized specimen into powder to (2) initial aqueous extraction of the pellet with Milli-Q water, (3) organic extraction of the pellet with MeOH:DCM, (4) freeze-drying the extracted material, (5) dissolution of the freeze-dried extract with 80% MeOH, (6) evaporation of the 80% MeOH from the pellet before, (7) resuspension with 80% MeOH at a final concentration of 25 mg/1000 uL and transfer to HPLC vials for, (8) UPLC-HR-MS/MS analysis and (9), identification of molecules. 12

Figure 6: Graphs a-e show a section (RT 5-12.5 min) of the base peak intensity (BPI) chromatogram displaying spectra analyzed via UHPLC-HR-MS/MS with positive electrospray of the representative healthy specimens from each sponge genus. Each line represents a different genus: *Baikalospongia* (B_H1), *Lubomirskia* (L_H1, L_H2), *Rezinkovia* (R_H1), and *Swartschewska* (S_H1). The location of random peaks shared by specimens from the four genera are marked with prominent red boxes and their shared mass-to-charge ratio (m/z (H+)). The relative peak intensities are calculated in Table 2. 18

Figure 7: Graphs a-e show a section (RT 4-13 min) of the BPI chromatograms from the UHPLC-HR-MS/MS analysis of healthy (L_H1, L_H2) and unhealthy (L_U1, L_U2, L_U3) *Lubomirskia* sponge specimens. 20

Figure 8. Graphs a-c show a section (RT 4-13 min) of the BPI chromatograms from the UHPLC-HR-MS/MS analysis of healthy (R_H1) and unhealthy (R_U1, R_U2) *Rezinkovia* sponge specimens. 21

Figure 9: Graphs a and b show a section (RT 4-13 min) of the BPI chromatograms from the UHPLC-HR-MS/MS analysis of healthy (S_H1) and unhealthy (S_U1) *Swartschewska* sponge specimens. 22

Figure 10: Graphs a-h show a section (RT 4-13 min) of the BPI chromatograms from the UHPLC-HR-MS/MS analysis of healthy (B_H1) and unhealthy (B_U1, B_U2, B_U3, B_U4, B_U5, B_U6, B_U7) *Baikalospongia* sponge specimens. 23

Figure 11. Graphs a-c show a section (RT 4-13.5 min) of the BPI chromatograms from the UHPLC-HR-MS/MS analysis of biofilm specimens (BF_1, BF_2, BF_3). 24

Figure 12: The relative abundances of bacterial phyla in sponge and biofilm specimens. Different sponge genera and biofilm specimens are grouped together and separated with dashed lines. The healthy sponge specimens representing each genus are highlighted on the x-axis. Bubble size corresponds to relative abundance percentage (%). The different disease

symptoms, detailed in Appendix 1, associated with the diseased sponges are represented above the relevant specimens, with the legend in the top right.....	28
Figure 13: a) The relative abundance of cyanobacterial orders in sponge and biofilm specimens. Different sponge genera and biofilm specimens are separated by dashed lines. The healthy sponge specimens from each genus are highlighted on the x-axis. b) The relative abundance of cyanobacterial genera in sponge and biofilm specimens. Different genera and biofilm specimens are separated by dashed lines. The healthy sponge specimens representing each genus are highlighted on the x-axis. Bubble size corresponds to relative abundance percentage (%). The different disease symptoms, detailed in Appendix 1, associated with the diseased sponges are represented above the relevant specimens, with the legend in the top right.	30
Figure 14: The relative abundance of Proteobacteria orders in sponge and biofilm specimens. Different sponge genera and biofilm specimens are separated by dashed lines. The healthy sponge specimens representing each genus are highlighted on the x-axis. Bubble size corresponds to relative abundance percentage (%).	31
Figure 15: The relative abundance of Bacteroidetes orders in sponge and biofilm specimens. Different sponge genera and biofilm specimens are separated by dashed lines. The healthy sponge specimens representing each genus are highlighted on the x-axis. Bubble size corresponds to relative abundance percentage (%).	32
Figure 16: Non-metric multidimensional scaling (NMDS) plot of dissimilarities between healthy sponge, unhealthy sponge, and biofilm specimens. The colored dots represent individual ASVs, with their associated phylum indicated by the colors presented in the legend. The plot was generated using the Bray-Curtis dissimilarity matrix using data that underwent square root transformation and Wisconsin double standardization. The stress value indicates the goodness of fit of the model, with 0 indicating a perfect fit and <0.1 a great fit.	33
Figure 17: Examples of fragmentation patterns of molecules from Table 2 (Left) and a screenshot of the results of using the Discovery tool in UNIFI 1.9.4 software to elucidate the molecule's identity (Right).....	56
Figure 18: Examples of fragmentation patterns of molecules from Table 3 (Left) and a screenshot of the results of using the Discovery tool in UNIFI 1.9.4 software to elucidate the molecule's identity (Right).....	57
Figure 19: Screenshot of a part of the identified compound list for <i>Lubomirskia</i> specimens (including L_H1, L_H2, L_U1, L_U2, L_U3) from molecular networking. Retrieved from Global Natural Products Social Molecular Networking (https://gnps.ucsd.edu).	58

Figure 20: An example of how molecules cluster together to form families in molecular networking. This cluster contains molecules associated with pheophorbide a in *Lubomirskia* specimens (including L_H1, L_H2, L_U1, L_U2, L_U3). The colors of the nodes (circles) indicate the proportions of the numbers of spectra detected of each molecule in the different specimens. The m/z (H+) of the molecules are listed next to each node and relationships between nodes and nodes groups are represented by the lines with arrows. Retrieved from Global Natural Products Social Molecular Networking (<https://gnps.ucsd.edu>). 59

Figure 21: a) The relative abundances of the bacterial communities at phylum level in lesion sites from L_U1, B_U2, and B_U4. b) The relative abundances of the cyanobacteria genera in lesion sites from L_U1, B_U2, and B_U4. 60

Abstract

Widespread mortality and disease are recognized as growing problems in benthic marine coral and sponge communities across the globe and despite being extensively studied, in most cases the etiology of disease remains unknown. Since 2011, sponge communities in freshwater Lake Baikal, Siberia, Russia have been affected by an unknown agent of disease, which has been causing an array of physical disease manifestations. Unusual microbial patterns have also been noted in the lake, including cyanobacterial bloom development and cyanobacterial biofilm growth on sponges, which have concurrently occurred with the overall decline of sponge communities. We used UPLC-HR-MS/MS and 16S rRNA sequencing to profile healthy and diseased sponges in order to elucidate the role of cyanobacteria in the development of sponge disease. Diseased specimens from the four sponge genera found in the littoral zone, encompassing a broad range of disease manifestations from violet-brown spots and bacterial biofilms to bleaching, were investigated. Within the four sponge genera, we discovered slight intergenera differences between microbial community composition (at the phylum and cyanobacterial genus levels) and metabolic output in the healthy representatives. As expected, most diseased sponges showed differences in their microbial community composition (at the phylum and cyanobacterial genus levels) and metabolic profiles in comparison to their healthy counterparts, and some connections could be drawn within sponges exhibiting similar disease symptoms. Though the association between cyanobacteria and disease etiology was not supported by the results of the metabolomic and metagenomic profiling and cyanotoxins were not discovered, this thesis provides a solid foundation for the ongoing, more in-depth study of the changes occurring in the Lake Baikal littoral sponge community.

Keywords: Lake Baikal, metabolomics, metagenomics, sponges, sponge disease

Abbreviations

Amplicon sequence variant (**ASV**)

Boiling point (**BP**)

Base peak intensity (**BPI**)

Degrees Celsius (**°C**)

Dissolved organic carbon (**DOC**)

Dichloromethane (**DCM**)

Dark spot syndrome (**DSS**)

Ethanol (**EtOH**)

Global Natural Products Social Molecular
Networking (**GNPS**)

High microbial abundance (**HMA**)

High-performance liquid chromatography
(**HPLC**)

Kilovolts (**kV**)

Liter per hour (**L/h**)

Low microbial abundance (**LMA**)

Lysophospholipid (**LPL**)

Mass-to-charge (**m/z**)

Methanol (**MeOH**)

Milliliter (**mL**)

Non-metrical multidimensional scaling
(**NMDS**)

Non-ribosomal peptide synthase (**NRPS**)

Platelet-activating factor (**PAF**)

Polyketide synthase (**PKS**)

Particulate organic carbon (**POC**)

Revolutions per minute (**RPM**)

Ribosomal ribonucleic acid (**rRNA**)

Retention time (**RT**)

Time-of-flight (**Tof**)

Total ion chromatogram (**TIC**)

Ultra-performance liquid chromatography
high-resolution mass spectrometry
(**UPLC-HR-MS/MS**)

Acknowledgements

Thank you to my supervisor, Anton Liaimer, for the guidance during the duration of this thesis. Thank you to Espen Hansen for letting us use the mass spectrometry facilities at Marbio and the very helpful supervision during the mass spectrometry analysis.

Thank you, Irina Tikhonova, Andrei Krasnopeev, and other staff members of the Limnological Institute of the Siberian Branch of the Russian Academy of Sciences in Irkutsk, Russia for their willingness to collaborate on this project. I am particularly grateful to the scuba divers for collecting the specimens in this study, Irina for her work with the specimens, and Andrei for processing the metagenomic data and R tips.

A huge thank you to Bente Lindgård for all of the tips on how to properly handle samples for mass spectrometry and her kindness, patience, and guidance during lab work.

Thank you to all of my friends, former coworkers, and family for the support in moving to Norway to do my Masters. Thank you to all of the friends I've made here for making me believe that was a very good decision!

1 Introduction

1.1 The Largest Freshwater Lake in the World

Located in southeastern Siberia, Russia, lies the largest, by volume, and deepest freshwater lake in the world (**Figure 1**). Lake Baikal contains over 20% of the Earth's fresh surface water supply (Moore et al., 2009) and sustains various macro-and microorganismal lifeforms, a majority of which are endemic to the lake (Beeton, 1984).



Figure 1: The approximate location and size of Lake Baikal within Siberia, Russia, which is surrounded by a black box. Figure retrieved from Khanaev et al., 2017.

The Russian environmental movement fought for the protection of Lake Baikal in the mid-20th century, understanding its importance as a source of drinking water for humans and unique ecosystem for animal and plant life (Weiner, 2002). Though finally designated a UNESCO World Heritage site in 1996, anthropogenic influences had already begun to reshape the Lake Baikal ecosystem. The construction of the Irkutsk hydropower station in the 1900s triggered a rise in water level, morphing shorelines and creating shallow zones of eutrophication surrounding the lake. A pulp and paper plant polluted the lake for almost 60 years before it was closed in 2013. Leftover production waste still enters the lake through groundwater (Bychkov et al., 2018). Efforts to protect Lake Baikal from more damaging industrial development are still ongoing, as propositions for the building of oil pipelines,

uranium enrichment plants, and bottled water plants alongside the lake continue to be suggested.

Currently, untreated wastewater is the most significant and unmanaged cause of eutrophication in Lake Baikal. Industrial and domestic wastewater is released into the lake, full of substances containing nitrites, nitrates, organic phosphorous, and sulfates, which are known triggers of eutrophication. Tourism, a growing industry, compounds this problem due to nonexistent centralized water and waste disposal facilities in recreational areas (Bychkov et al., 2018). In addition to localized anthropogenic influence, evidence for climate change at Lake Baikal is now deemed “abundant.” Decreasing ice thickness and higher amounts of precipitation, in addition to increasing air temperature, are irrefutable markers of the changes that have swept through this region in the last century (Moore et al., 2009). Since 2011, abnormal changes in vital benthic community members have been observed. It is clear that monitoring the unique ecosystem of Lake Baikal is imperative to understanding and conserving its future.

1.2 The Sponge Holobiont

Sponges, similar to corals, are fundamental to benthic marine and freshwater communities. Outwardly simple in morphology and structure, they are considered invertebrate animals of the phylum Porifera, and perform integral functions in diverse ecosystems (Renard et al., 2013). Though the mechanism of the emergence of multicellularity from unicellular organisms is still debated (Sebé-Pedrós et al., 2017), the “Porifera-first” hypothesis in which poriferans are the sister group of other metazoans is largely accepted (Simion et al., 2017). The composition of their skeleton and body form largely determines if they are in the Hexactinellida, Demospongiae, Calcarea, or Homoscleromorpha clades (Renard et al., 2013). The majority of sponges belong to the most widespread and diverse class Demospongiae (Morrow & Cárdenas, 2015), including sponges of the endemic *Lubomirskiidae* family in Lake Baikal.

Sponge structures vary from what appears to be a simple tube (asconoid) to a more compartmentalized and complex chamber (syconoid and leuiconoid) (**Figure 2**), though their roles are more or less the same (Hogg et al., 2010). Sponges are involved in the cycling of nutrients and organic matter (Reiswig, 1971, Diaz & Ward, 1997), play a significant role in benthic-pelagic coupling (Pile & Young, 2006), and host different varieties of water-dwelling invertebrates (Haygood et al., 1999, Macdonald et al., 2006).

Their role, particularly in the food chain and cycling of organic carbon, cannot be understated. Oceans are the largest reservoir of cycled dissolved carbon on Earth (Hedges, 1992). Approximately 70% of the sponge diet is composed of dissolved organic carbon (DOC), which they convert into particulate organic carbon (POC). Filtered POC is then consumed by other benthic organisms and eventually cycled through higher trophic levels (Mcmurray et al., 2016). Their role in nitrogen cycling is similarly important and complex, and the same species of sponge has been found to host different steps of the nitrogen cycle (Hoffmann et al., 2009, Li et al., 2014). Sponges also feed on bacteria (Reiswig, 1975) and are fed on by predators including parrotfish (Dunlap & Pawlik, 1998). Known for their symbiotic interactions with microorganisms, they are hosts to diverse communities of unicellular algae, fungi, cyanobacteria, and heterotrophic bacteria (Webster, 2007).

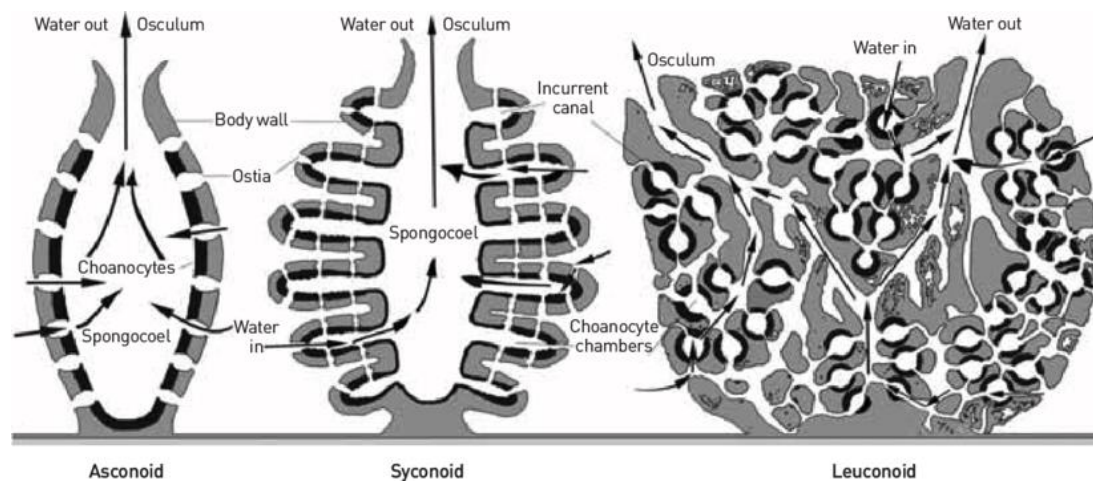


Figure 2: Image of the three types of sponge structures with some labelled parts of the body. Arrows indicate the flow of water through the chambers of the different structures. Demosponges generally have the most complex body structure (leuconoid). Figure retrieved from Hogg et al., 2010.

Demosponges, belonging to class Demospongiae, lack traditional tissues or organs and are instead organisms composed of multilayered cells. Most have a leuconoid body structure. The outer layer, known as the pinacoderm, encapsulates the second layer, the choanoderm, which separates the inner chambers of the sponge from surrounding water and contains cells responsible for capturing food particles. A matrix infused with spongin and collagen proteins separates these two layers of cells and gives the demosponge a sort of skeletal build (Hentschel et al., 2003). Symbiotic prokaryotes and eukaryotes form communities within these tissue layers and amongst amoeboid sponge cells. Up to 40% of a sponge's body mass has been determined to be composed of sponge microbiome members, though this amount varies due to differences between species morphologies and environmental and geographical factors (Vacelet & Donadey, 1977).

Differences in microbial abundance in marine demosponges points to the evolution of two distinct survival strategies: one heavily incorporating symbiont microorganisms and the other one not. Sponges with low microbial abundance (LMA) host a similar number of microorganisms as the surrounding seawater while sponges with high microbial abundance (HMA) have 2-4 orders of magnitude higher amounts (Hentschel et al., 2003). LMA and HMA sponges have distinct morphological and physiological features, which suggests that microorganisms play an important role in sponge evolution (Weisz et al., 2008).

Sponges have fairly advanced immune systems. They are sessile organisms vulnerable to predation, which makes the evolution of a molecular defense system prudent. Immune molecules with high sequence similarities to members of other metazoan phyla (Müller et al., 1999) and activation of immune response kinases in response to bacterial endotoxin exposure (Böhm et al., 2001) are elements of immune response that have been conserved from sponges to humans. Bacterial symbionts are able to avoid becoming the targets of host sponge immune response. Additionally, they are also able to avoid being digested by their hosts, when compared to non-symbiotic bacteria, though the mechanisms for how they achieve that are still under speculation (Wilkinson et al., 1984, Hentschel et al., 2012).

Another aspect of the sponge defense system is the production of antimicrobial compounds. Sponges are the most prolific source of natural products in the marine environment, and many of those products can be attributed to their symbiont microbial communities, as evidenced by their structural similarities to molecules associated with bacteria (Laroche et al., 2007, Blunt et al., 2011). Other natural products, based on their structural similarities, point to eukaryotes such as dinoflagellates and fungi as the origin (Hentschel et al., 2012). Unson and Faulkner (1993) first proved that isolated polychlorinated compounds were produced by a cyanobacterial species on marine sponge *Dysidea herbacea*, rather than by the sponge itself. Since then, natural products have been isolated from both marine and freshwater symbiont cyanobacterial communities (Blunt et al., 2018, Ishida & Murakami, 2000).

1.3 Cyanobacteria and Their Natural Products

Cyanobacteria is an ancient phylum that emerged over 2 billion years ago, according to fossil record (Rasmussen et al., 2008). Cyanobacteria are known as aerobic photoautotrophic microorganisms that carry out photosynthetic processes via photopigments e.g. chlorophyll *a* and phycobiliproteins (Waterbury, 2006). However, they are

metabolically diverse and impressively capable of adaptation, for instance to anoxic and dark growth conditions (Stal, 1995). In fact, many cyanobacteria are heterotrophic microorganisms and are simultaneously able to perform photosynthesis and fix dinitrogen in special cells known as heterocysts.

Cyanobacteria is a phylum of great diversity, due to its member's adaptive abilities. In addition to diverse metabolisms, cyanobacteria have diverse morphologies and growth patterns, and are found in diverse environments around the world (Castenholz et al., 2001). They also harbor diverse relationships with the prokaryotic and eukaryotic organisms around them. Cyanobacteria utilize sponges as sources of nitrogen and carbon while exporting supplemental nutrients to sponge tissue (Wilkinson & Fay, 1979). When environmental conditions are balanced, this relationship remains stable and both organisms benefit. However, changes in the environment can trigger changes within cyanobacterial communities that can be detrimental to the sponge and cause tissue damage or death, marked by distinct discoloration (Rützler, 1988).

Cyanobacteria, in addition to being known for their roles as nitrogen and carbon fixers, are notorious producers of secondary metabolites. The production of secondary metabolites is specific to certain strains of cyanobacteria, and there is a large amount of variation both between and within species (Kurmayer & Christiansen, 2009). Not all cyanobacteria are created equal. Filamentous and heterocystous strains tend to contain larger amounts of non-ribosomal peptide synthase (NRPS), polyketide synthase (PKS), or NRPS/PKS hybrid domains in comparison to unicellular strains, which are unable to form heterocysts (Ehrenreich et al., 2005).

Secondary metabolites are, as one can guess, highly diverse classes of peptides. Classes include aeruginosins, microcystins, nodularins, and nostocyclopeptides, and the list of natural products isolated from cyanobacteria continues to grow (Carmichael, 1992, Golakoti et al., 2001, Tidgewell et al., 2010). Some act as toxins to eukaryotic organisms and multiple potent cyanotoxins can be released in cyanobacterial blooms (Casero et al., 2019). Cyanotoxins are largely classified by their effect on human health (e.g., hepatotoxins, neurotoxins) though, of course, they are harmful to a wide variety of living organisms (Carmichael, 1992). Due to their benefit or risk to human health there is a distinct disparity in tone between the findings of secondary metabolites from cyanobacteria in marine versus freshwater environments, i.e.,

the mining of marine cyanobacteria for novel compounds for use in medicine versus the evaluation of risk from secondary metabolite toxicity (Tidgewell et al., 2010).

1.4 Sponge Disease History, Globally and Locally

Lake Baikal contains sponges spanning four known genera of order Spongillida (Itskovich et al., 2015), which altogether compose 44% of the benthic biomass of Lake Baikal (Pile et al., 1997). The year 2011 marked the beginning of an observed, rapid decline of several sponge species in the littoral zone of the lake (Belikov et al., 2018). Initially, the affected sponges exhibited areas of abnormal pink-colored discoloration. Healthy sponges of the *Baikalospongia* and *Lubomirskia* genera, which are the most common genera of endemic sponges found in the lake, are typically a vibrant green due to associated symbiont dinoflagellates (Annenkova et al., 2011). Healthy sponges of the *Lubomirskia* genus are also green due to symbiosis with green algae *Mychonastes* (Chernogor et al., 2013). In 2013 the disease appeared to diversify in physical appearance and brown or violet spots, in addition to discolored zones and entirely bleached and necrotic sponges, became common (Belikov et al., 2019). In present day, the different physical presentations of disease and bleaching are persistent in Lake Baikal sponge communities.

The incidence of mass disease events in sponges is not a new phenomenon, though this is the first observed case in a freshwater environment (Belikov et al., 2018). Mass disease and mortality events involving sponges have been investigated in several marine environments including the Maldives (Sweet et al., 2015), western Mediterranean Sea (Cebrian et al., 2011), Key Largo, Florida (López-Legentil et al., 2010), and Caribbean Sea (Angermeier et al., 2012). The etiologies of these diseases have ranged from undetermined, to most likely caused by a single organism, or two organisms acting in concert with each other.

A novel alphaproteobacteria was the first pathogen to be directly implicated in causing spongin tissue necrosis in the Great Barrier Reef (Webster et al., 2002). In the Caribbean, it was unclear if an alphaproteobacteria found in samples exhibiting sponge white patch disease was an opportunistic pathogen or cause of the disease (Angermeier et al., 2012). Later, Sweet et al., (2015) demonstrated the second confirmed instance of sponge disease linkage to specific pathogens. An inoculation of both a bacteria *Rhodobacteraceae* species and fungi *Rhabdocline* replicated the pathology seen in marine sponges in the Maldives. Though it ultimately did not meet Henle-Koch's postulates for its role in causing the

aforementioned sponge disease, another bacterium tested in this study was the cyanobacteria *Hormoscilla spongelliae* (Oscillatoriales).

Cyanobacteria have previously been associated with sponge disease and necrosis. In Rützler, 1988, it was suggested that overgrowth of cyanobacteria caused sponge histolysis in the Caribbean. Cyanobacterial blooms and the widespread death of multiple sponge species were concurrently observed in Florida Bay, USA, which the authors suggested was due to release of overwhelming amounts of toxins by the cyanobacteria (Butler et al., 1995). An investigation into the etiology of *Aplysina* red band syndrome in Caribbean sponge communities indicated that an unknown cyanobacteria species accompanied the areas of distinct disease coloration. However, researchers were unable to implicate the cyanobacteria species with causing the disease and proposed that the cyanobacteria acted as an opportunistic pathogen after the disease was already established (Olson et al., 2006). The majority of these studies suggest that establishing clear relationships between sponge diseases and the organisms causing these diseases continues to challenge researchers.

The causative agent of the different manifestations of the diseased Lake Baikal sponges remains unknown though there is evidence that points to the involvement of cyanobacteria. Cyanobacterial toxins have recently been found in above average concentrations in different areas of Lake Baikal, coinciding with the appearance of diseased and necrotic sponges. Bioassays detected abnormal concentrations of microcystins near a tourist hotspot in 2013 and bacterioplankton sequencing revealed cyanobacterial dominance and the presence of two notorious toxin-producing genera (Belykh et al., 2015). Evidence of freshwater cyanobacteria species *Dolichospermum* (formerly *Anabaena*) *lemmermannii* was found at the site of a contaminated area near the Irkutsk hydroelectric power station dam, located along a river originating in Lake Baikal. Remnants of this cyanobacterial bloom were found amidst high nutrient levels and dangerously high concentrations of saxitoxin (Grachev et al., 2018). Microcystins emitted from benthic biofilms have also been found (Belykh et al., 2017).

Kaluzhnaya and Itskovich 2015 reported major changes in the microbiomes of bleached *Lubomirskia baikalensis* sponges in comparison to their healthy counterparts. Previous studies of the endemic sponges found that Actinobacteria, Bacteroidetes, and Proteobacteria were predominant in healthy specimens (Kaluzhnaya et al., 2012, Gladkikh et al., 2014). This was not the case in bleached specimens where the phylum Cyanobacteria, most of

which belonged to the *Synechococcus* genus, composed over a quarter of the bacterial community. Proteobacteria, Actinobacteria, and Verrucomicrobia also made up significant shares of the bleached bacterial community, in highest to lowest order.

Belikov et al., 2019 investigated the microbial communities of healthy and diseased *Lubomirskia* sponges from different years and found that symbiont communities in “dirtier” areas like Listvyanka were similar to those in healthier areas. The exception was a pink-colored specimen from the first appearance of disease in 2011, which was dominated by members of *Synechococcaceae* and completely devoid of algal symbiont *Choricystis sp.* When healthy sponge microbiomes from different years were compared to each other, a significant shift in the composition was noted from 2010 to 2015. Members of families associated with opportunistic pathogenesis increased in 2015 sponge specimens.

An earlier study analyzing biofilm diversity on stone substrates and steel in Lake Baikal detected sixteen species of cyanobacteria from Nostocales, Oscillatoriales, and Chroococcales and determined that they were “basic components of biofilms” (Sorokovikova et al., 2013). Cyanobacterial diversity in the sponge samples and biofouling were also the subjects of a more recent exploratory study of samples collected in 2014-2015. Using microscopy and 16S rRNA analysis, Sorokovikova et al., (2020) noted the emergence of several novel cyanobacterial species in these specimens. *Tolypothrix distorta* (Nostocales) became the dominant cyanobacterial species in diseased sponge samples and biofouling, when it was previously limited to benthic stony substrate environments. Species from genera *Tychonema* (Oscillatoriales) and *Symplocastrum* (Oscillatoriales) were, for the first time, found in the microbial communities in diseased sponges after being observed on rocky substrates in the littoral zone of the lake. Additionally, *Tychonema* flourished in sponge lesions.

Both *Tolypothrix distorta* and members of the *Tychonema* genus have been suspected or implicated in the production of secondary metabolites such as saxitoxin and anatoxin-a. Kleinteich et al., 2013 found bacteria that saxitoxin producing cyanobacterial mats had the highest 16S rRNA similarity to *Tolypothrix distorta*. Cytotoxic cyclic dodecapeptides tychonamide a and b (Mehner et al., 2008) and anatoxin-a (Shams et al., 2015) have been isolated from *Tychonema* species. During an investigation into the changing cyanobacterial communities of Lake Garda, 70% of *Tychonema* specimens contained genes tied to the production of various anatoxins and homoanatoxin-a (Salmaso et al., 2016). An increase in

anatoxin-a peak levels in Lake Garda since 2009 has been attributed to growing populations of *Tychonema bourrellyi*. Of course, these toxins are not produced by just these species of cyanobacteria. Saxitoxin, for instance, is produced by different cyanobacterial species in freshwater environments (Carmichael et al., 1997, Negri & Jones, 1995, Lagos et al., 1999, Pomati et al., 2000).

1.5 Thesis Aims

The unknown effects of changing bacterial communities living on Lake Baikal sponges, in conjunction with the fact that the sponges continue to suffer from disease outbreaks, was the impetus for this thesis. Cyanobacterial communities were the specific target of this investigation. The aims of this study were the following:

- I)** Use an untargeted metabolomics approach with a ultra-high performance liquid chromatography high-resolution mass spectrometry (UPLC-HR-MS/MS) system to compare the metabolic profiles of healthy and diseased sponges and cyanobacterial biofilms from Lake Baikal.
- II)** Understand the connection between differences in metabolic profiles and observed disease prevalence.
- III)** Identify the possible molecules of interest in the metabolic profiles, specifically those that have fragmentations patterns associated with cyanobacterial-associated secondary metabolites.
- IV)** Use metabolomic data in tandem with 16S rRNA metagenomic data to investigate the relationships between microbial community composition and metabolic activity in the sponges.

2 Materials and Methods

2.1 Specimen Procurement

All specimens processed and analyzed in this thesis were collected on December 9-10, 2017 from the littoral zone of Lake Baikal by our collaborators from the Limnological Institute of the Siberian Branch of the Russian Academy of Sciences in Irkutsk, Russia. Specimens were procured from three different sites, though eukaryotic biofilm specimens collected from Listvyanka are not investigated in this thesis (**Figure 3**).

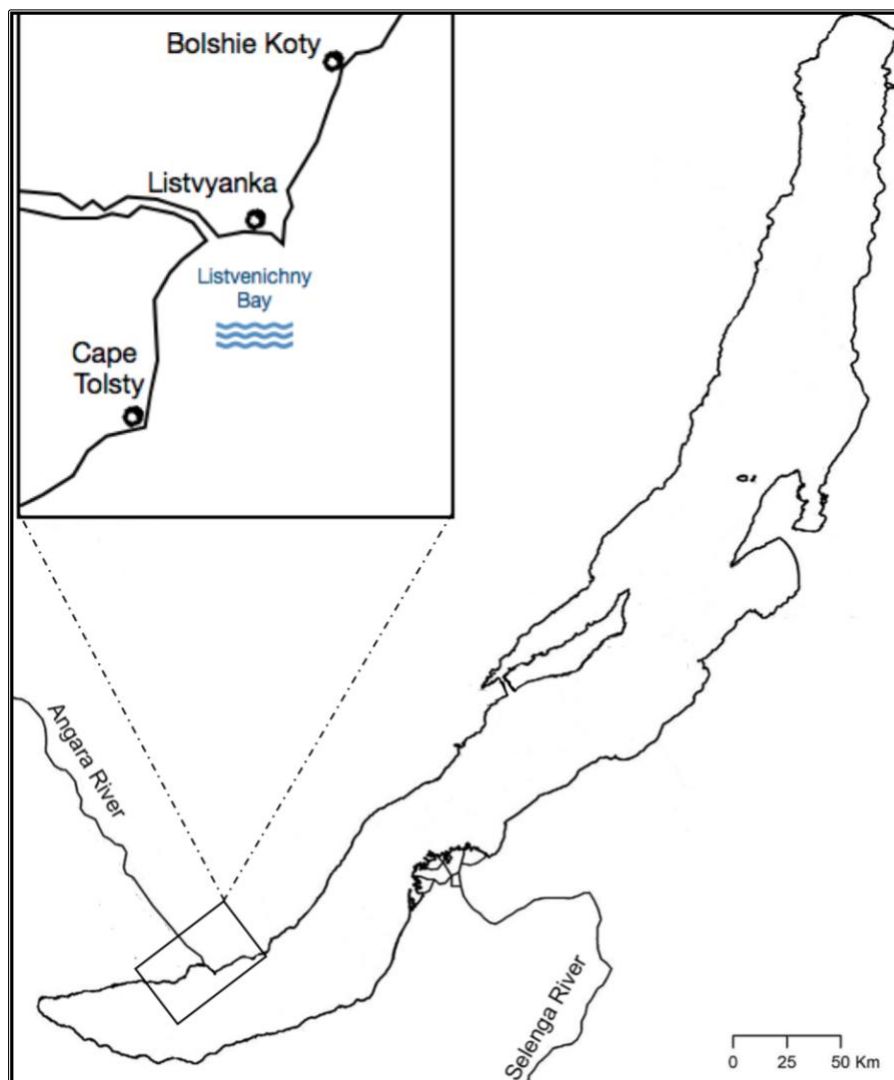


Figure 3: A map of Lake Baikal with the three specimen sites marked in the map insert in the top left corner. Sponges were collected from the littoral zone of the lake associated with the marked sites. The map was modified from Khanaev et al., 2017.

Healthy and diseased specimens from four different sponge species native to Lake Baikal were procured, as well as bacterial biofilms not physically associated with sponges. Diseased sponges were identified visually by the scuba diver. The presence of abnormal violet or

brown lesions, bacterial or fungal biofilms, or discolored or bleached areas on the body of the sponge indicated disease (**Figure 4**).



*Figure 4: Images from the scuba diving session for specimen collection. A healthy *Lubomirskia baikalensis* sponge is pictured in (a), an unhealthy bleached *Lubomirskia baikalensis* sponge is pictured in (b), and an unhealthy *Baikalospongia* sp. with an attached dark purple biofilm is pictured in (c). Images courtesy of Irina Tikhonova.*

Additionally, our collaborators from the Limnological Institute identified the sponge species and microscopically identified relevant associated bacterial or cyanobacterial species on the diseased specimens or isolated biofilm specimens. All images, collection site information, and disease descriptions we received about the specimens are in **Appendix 1**. After procurement and identification, the specimens were lyophilized and allocated into separate Petri dishes. The entire sponge body was lyophilized, though metabolites have been documented to accumulate in certain zones in sponges (Schupp et al., 1999, Furrow et al., 2003, Rohde & Schupp, 2011). Bioactive metabolites accumulate in the periphery of the sponge, rather than the center, as they act as forms of chemical defense (Schupp et al., 1999). The lyophilized specimens were transported to us at the University of Tromsø and stored at -20°C until extractions for mass spectrometry analysis began. A crude overview of the specimens and workflow for mass spectrometry analysis is detailed in **Figure 5**.

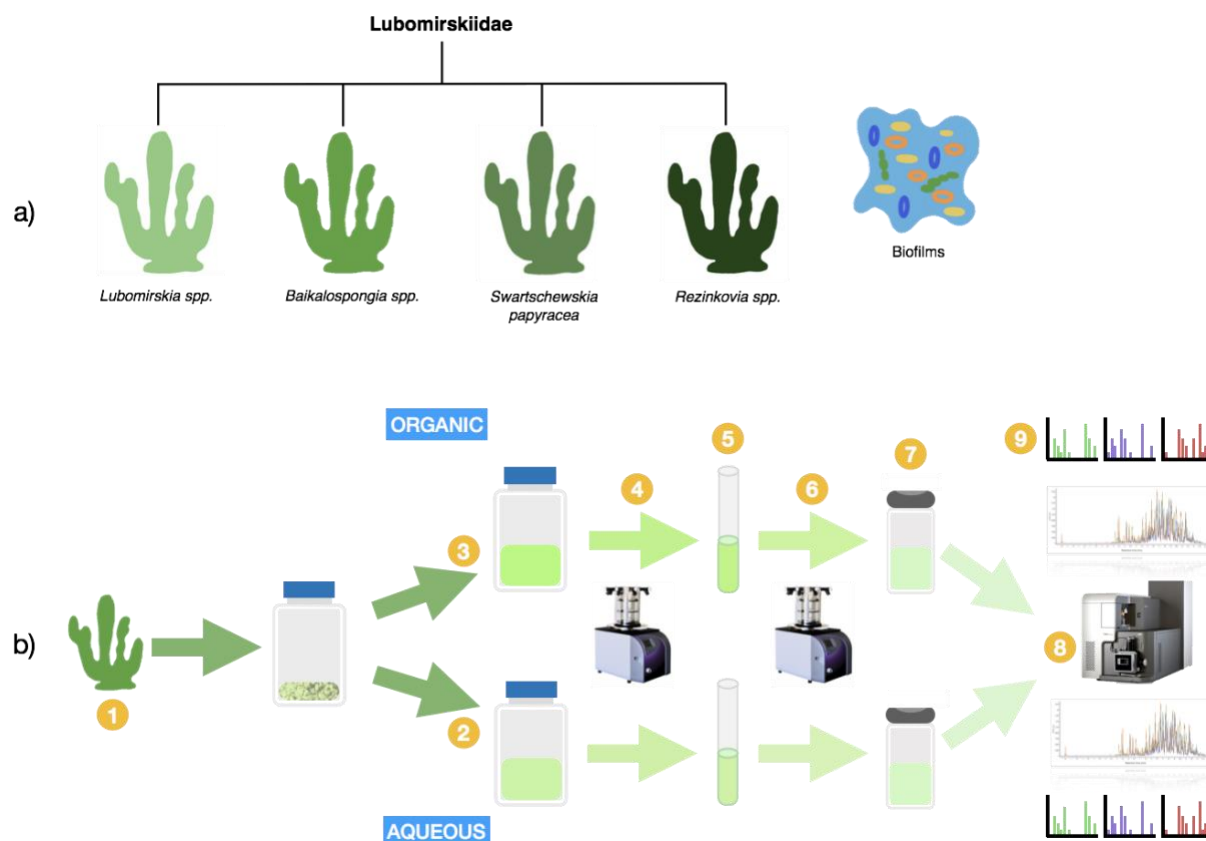


Figure 5: **a)** An overview of the specimens from four different genera in the Lubomirskiidae family of endemic Lake Baikal sponges and biofilm specimens unassociated with sponges. **b)** A simplified workflow of the process to extract mass spectrometry data from sponge and biofilm specimens. The steps for the organic extraction are labelled from (1) grinding down the lyophilized specimen into powder to (2) initial aqueous extraction of the pellet with Milli-Q water, (3) organic extraction of the pellet with MeOH:DCM, (4) freeze-drying the extracted material, (5) dissolution of the freeze-dried extract with 80% MeOH, (6) evaporation of the 80% MeOH from the pellet before, (7) resuspension with 80% MeOH at a final concentration of 25 mg/1000 μ L and transfer to HPLC vials for, (8) UPLC-HR-MS/MS analysis and (9), identification of molecules.

2.2 Extraction of Secondary Metabolites from Sponge and Biofilm Specimens

Though there are many mass spectrometry methods available, the utilization of ultra-performance liquid chromatography (UPLC) in tandem with time-of-flight (ToF) mass spectrometry allows for particularly efficient separation, assessment, and metabolic profiling of specimens (Wolfender et al., 2010). The sophisticated mass spectrometry facilities available at Marbio gave us the ability to analyze the specimens via an untargeted metabolomics approach.

The lyophilized specimens underwent an aqueous extraction, followed by an organic extraction, as outlined in the Extraction of Marine Invertebrates protocol provided by Espen Hansen from Marbio. Specimen weights were noted before they were ground into fine powder using sterilized ceramic mortars and pestles. Some specimens necessitated the addition of

liquid nitrogen for flash freezing before being ground into a powder. The sterilization of spatulas and work area with ethanol, to avoid contamination in between specimens, was consistently done. Once ground down, specimens were transferred into Duran bottles that had been autoclaved and triple washed with distilled water, and stored at -20°C.

2.2.1 Aqueous Extraction

Milli-Q water (Merck) was added to each specimen in a 1:10 weight to volume ratio, based on their initial weights. Specimen BF_3, due to its small weight and stickiness, was rinsed from the mortar and pestle using a larger volume of Milli-Q water than prescribed by the 1:10 ratio. All specimens were extracted at 4°C on a shaker set to approximately 75 (Mot 1/min) for 3 hours, with manual shaking occurring every hour. The dissolved specimens were poured into 50 mL centrifuge tubes (VWR) and centrifuged at 4600 rpm for 30 min at 5°C. The supernatants from the specimens were carefully poured back into their respective Duran bottles, without dislodging the pellets in the tubes. The centrifuge tubes with the pellets were stored at -20°C for the organic extraction. The caps of the Duran bottles containing the supernatants were removed, covered with parafilm with several holes to ensure exposure to vacuum, and freeze-dried using manual mode on the VirTis BenchTop Pro with Omnitronics (SP Scientific). The specimens were freeze-dried under vacuum at temperatures below -100°C for 24-97.5 hours, times varying with each specimen. The freeze-dried aqueous extracts were stored at -20°C until mass spectrometry sample preparation began.

2.2.2 Organic Extraction

The caps of the centrifuge tubes containing the pellets set aside for the organic extraction were partially unscrewed and the pellets were freeze-dried using manual mode on the VirTis BenchTop Pro. Finished specimens were stored at -20°C and new Duran bottles were autoclaved and rinsed in preparation for the organic extractions. Specimens were transferred from the centrifuge tubes to the Duran bottles and their weights were recorded. Equipment for the organic extractions was rinsed with 96% EtOH or MeOH before use.

A 1:1 methanol:dichloromethane (MeOH/DCM) (Merck Millipore/Sigma-Aldrich) solution was added to the specimens in a 1:10 weight to volume ratio. The pellet from specimen BF_3, again, due to its small size, was dissolved in a larger amount of 1:1 MeOH/DCM solution than suggested in the protocol. Pellets were extracted overnight on a shaker in a cold room ranging from 5-7°C. The extracted solutions were filtered through a Büchner funnel with inlaid Whatman qualitative filter paper, Grade 3 (Merck Millipore) before being transferred to

Duran bottles. After the first round of collection, the pellets were extracted again in the cold room for 1-2 hours using a 1:5 weight to volume ratio of 1:1 MeOH/DCM solution. The extracted solutions from the second round were filtered through the same Büchner funnel with inlaid Whatman paper and added to the extractions from the first round.

The specimen filtrates were transferred to centrifugal tubes fitted for the Genevac EZ-2 Elite Personal Evaporation (SP Scientific) for evaporation. The Very Low BP (Boiling Point) program with preset settings was used for the evaporation of the majority of the specimens. The Low BP program was used to evaporate remaining MeOH in a few samples at a faster rate than the Very Low BP program. Specimen evaporation times ranged from 3-4.5 hours. Evaporated organic extract specimens were stored at -20°C before being used for mass spectrometry sample preparation.

2.2.3 Mass Spectrometry Sample Preparation

Thin centrifuge tubes were rinsed with 80% MeOH, labelled, and weighed in preparation for aqueous and organic sample evaporation. 4 mL of 80% MeOH was used to dissolve the organic extraction samples and an additional 1 mL of 80% MeOH was used to rinse the centrifuge tubes. 4 mL of 50% MeOH was used to dissolve the aqueous extraction samples, with an additional 1 mL used to rinse the Duran bottles. Approximately 5 mL of partially dissolved samples were collected for evaporation in the thin centrifuge tubes. They were evaporated using the SpeedVac® Plus SC210A (Savant) and attached Refrigerated Vapor Trap (Savant) for 5.5-9 hours.

After evaporation, the dry weights of the specimens were calculated. The aqueous and organic samples were dissolved in 50% MeOH and 80% MeOH, respectively, at a ratio of 25 mg/1000 uL. Either 200 or 500 uL of the dissolved specimens were transferred to Eppendorf tubes and centrifuged at 13000 rpm for 5 min. 150 or 400 uL of the supernatant was carefully transferred into HPLC vials and used for further mass spectrometry analysis. Specimens were stored at -20°C.

2.3 Mass Spectrometry

The extracts were analyzed via UHPLC-HR-MS/MS. The mass spectrometry system was composed of a Waters Acquity I-Class UPLC System (Milford, MA, USA) equipped with a PDA Detector and VION IMS QToF Mass Spectrometer (Waters). The UPLC was outfitted with a 1.7 um Acquity UPLC BEH C18 (2.1 x 100 mm) column (Waters). Molecules were

ionized with electrospray (ESI), used in positive mode, and the mass spectrometer was used with the standard operating conditions detailed in **Table 1**. The step gradient used ranged from 90:10 water:acetonitrile to 10:90 water:acetonitrile over 13.5 min. The range of masses detected were m/z 50-2000.

Table 1: Operating conditions of the VION IMS QTof Mass Spectrometer.

Capillary Voltage	0.80 kV
Desolvation Gas Flow Rate	800 L/h
Cone Gas Flow Rate	50 L/h
Desolvation Temperature	350 °C
Source Temperature	120 °C

UNIFI 1.9.4 software was used during data acquisition and analysis (Waters). Molecules were dereplicated and identified using the Discovery tool and ChemSpider databases, in addition to fragmentation patterns found in other papers.

2.4 Metagenomic Analysis

Andrei Krasnopeev and Irina Tikhonova, from the Limnological Institute, extracted, amplified, and sequenced (Illumina) 16S rRNA from corresponding pieces of the specimens they sent us for mass spectrometry extraction and analysis. Krasnopeev and Tikhonova performed sequence processing, quality filtering, chimera removal and clustering in Amplicon Sequence Variants (ASVs) of 16S rRNA gene fragment libraries using the following *DADA2* package for R (Callahan et al., 2016) tutorial (<https://benjjneb.github.io/dada2/tutorial.html>). The data we received was an Excel table containing ASV read counts. Sequences of eukaryotic origin (e.g. chloroplasts) were manually removed. Sequences belonging to cyanobacteria were analyzed via the NCBI (National Center for Biotechnology Information) BLAST (<http://www.ncbi.nlm.nih.gov/blast/>) and Michigan State University RDP (Ribosomal Database Project) (<http://www.rdp.cme.msu.edu/>). NCBI taxonomy was used to classify the cyanobacterial sequences. To quantify relative abundances, the read counts were normalized and calculated as a percentage of the total sample.

2.5 Statistical Analysis

RStudio 1.3.959 (R Core Team, 2018) was used for data analysis of metagenomic data. In particular, the function *metaMDS* in package *vegan* (Oksanen et al., 2019) was used to perform non-metrical multidimensional scaling (NMDS) of the ASVs associated with assigned sequences. Bray-Curtis distance dissimilarities between sponge and biofilm specimens were generated using square root transformed and Wisconsin double standardized ASVs and plotted. The package *ggplot2* (Wickham, 2016) was used to generate relative abundance bubble plots using the metagenomic data.

Results

2.6 UHPLC-HR-MS/MS Metabolic Profiling

Organic and aqueous extracts from the sponge and biofilm specimens went through metabolic profiling using UHPLC-HR-MS/MS with positive electrospray. Some aqueous extracts formed a precipitate during storage at -20°C, which compromised the integrity of the aqueous specimen results. Therefore, only the results of the organic (MeOH:DCM) extract profiling will be presented. **Figures 6-11** contain base peak intensity (BPI) chromatograms for the organic extracts of the sponge and biofilm specimens. BPI chromatograms detect the most intense peak at each point on the spectrum. They were used for analysis, rather than total ion chromatograms (TIC), in order to reduce background noise.

Molecules detected by UHPLC-HR-MS/MS are presented in **Table 2** and **Table 3**. We attempted to dereplicate these molecules using the available databases included in the ChemSpider molecular library. The fragmentation patterns of peaks matching molecules from the databases were analyzed to confirm the match. In all cases, the molecules had multiple matches or were unidentified. Most of the structures of the “identified molecules” in **Table 2** and **3** are therefore unconfirmed. Examples of fragmentation patterns of molecules listed in **Table 2** can be found in **Appendix 2: Figure 17**. Examples of fragmentation patterns of molecules listed in **Table 3** can be found in **Appendix 2: Figure 18**. Molecular ions associated with the fragmentation patterns associated with specific cyanotoxins were also utilized in the search for cyanobacterial secondary metabolites.

Raw mass spectra files from all organic extraction samples were converted into 32-bit files with the MSConvert tool from ProteoWizard (Holman et al., 2014). These files were uploaded to the Global Natural Products Social Molecular Networking server (Wang et al., 2016), where related molecules from the sponges and biofilms were clustered into families (Frank et al., 2007).

2.6.1 Healthy Sponge Comparative Chromatograms

In **Figure 6**, segments from the metabolic profiles of the five visually healthy sponge specimens between retention time (RT) 5-12.5 min are displayed. This segment is representative of the overall chromatogram, which shows a general similarity between the different specimen’s metabolomes. Though some peaks have larger detection counts in certain specimens, the most prominent peaks have similar relative peak intensities. The specimen

whose metabolic profile appears to slightly stand out from the others belongs to the *Rezinkovia* genus. This is confirmed by calculating the relative peak intensities of randomly selected prominent peaks in **Figure 6**. As calculated in **Table 2**, *Swartschewskia*, *Lubomirskia*, and *Baikalospongia* healthy sponges share their most prominent peak, which has a m/z (H^+) 496.3 (RT 9.2 min). The most prominent peak associated with the healthy *Rezinkovia* specimen is m/z (H^+) 482.3 (RT 8.7), which the other specimens have slightly lower levels of. R_H1 has other, slightly less prominent, relative peak intensities in common with L_H1, L_H2, and S_H1, when compared to B_H1. The metabolic profiles of L_H1 and L_H2, which are replicates from the same *Lubomirskia* specimen, show that there is little variation in between samples from the same specimen. This indicates a fairly consistent distribution of metabolites and that the metabolic profiles of our specimens are more or less representative of the entire specimen.

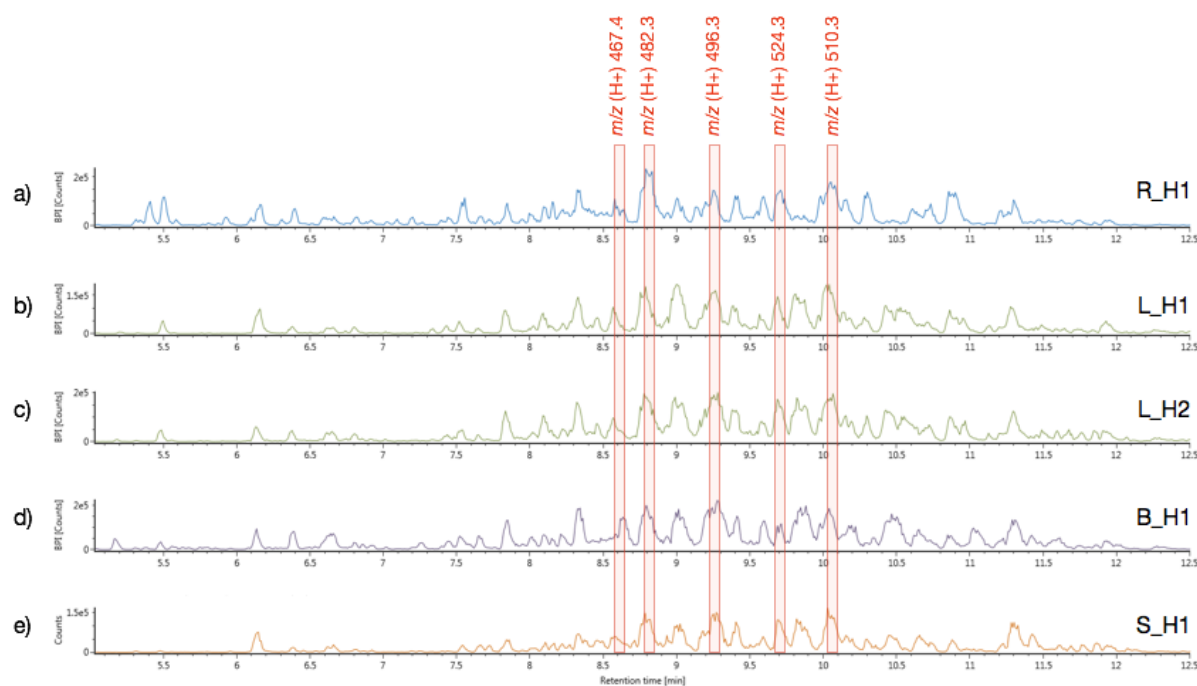


Figure 6: Graphs a-e show a section (RT 5-12.5 min) of the base peak intensity (BPI) chromatogram displaying spectra analyzed via UHPLC-HR-MS/MS with positive electrospray of the representative healthy specimens from each sponge genus. Each line represents a different genus: *Baikalospongia* (B_H1), *Lubomirskia* (L_H1, L_H2), *Rezinkovia* (R_H1), and *Swartschewskia* (S_H1). The location of random peaks shared by specimens from the four genera are marked with prominent red boxes and their shared mass-to-charge ratio (m/z (H^+)). The relative peak intensities are calculated in Table 2.

Dereplication of even these very prominent peaks was challenging, as seen in **Appendix 2: Figure 17b, c**. Generally, in cases of multiple matches using the Discovery tool, the matched molecules had the same elemental compositions, i-FIT confidence percentages, and spectral fragmentation patterns. Conversely, m/z (H⁺) 467.4 (RT 8.5) in **Appendix 2: Figure 17a** had only one match with a molecule in the ChemSpider databases with 100% i-FIT confidence.

Table 2: The relative peak intensities (%) of the molecules annotated in Figure 6, displaying similarities and differences between the metabolic output of healthy sponge specimens of different genera.

m/z (H⁺)	RT	<i>R_HI</i>	<i>L_HI</i>	<i>L_H2</i>	<i>S_HI</i>	<i>B_HI</i>
467.4	8.5	71.9	35.6	39.5	62.6	32.1
482.3	8.7	100	89.8	93	92.7	76.3
496.3	9.2	49.8	100	100	100	100
524.3	9.6/9.7	57.2	50.7	55.2	61.8	26.6
510.3	10	81.3	87.1	84.9	87.9	53.9

2.6.2 Healthy Versus Unhealthy Sponge Chromatograms

Figure 7 displays the segments of metabolic profiles of the healthy and unhealthy *Lubomirskia* specimens between RT 4-13 min. The healthy specimens, L_H1 and L_H2, appear to share prominent peaks with L_U2 and L_U3. However, L_U1 overall has noticeably lower peak intensities compared to the healthy and other unhealthy specimens. A selected number of peaks that are detected at higher levels in L_U1 are discussed in **Table 3**.

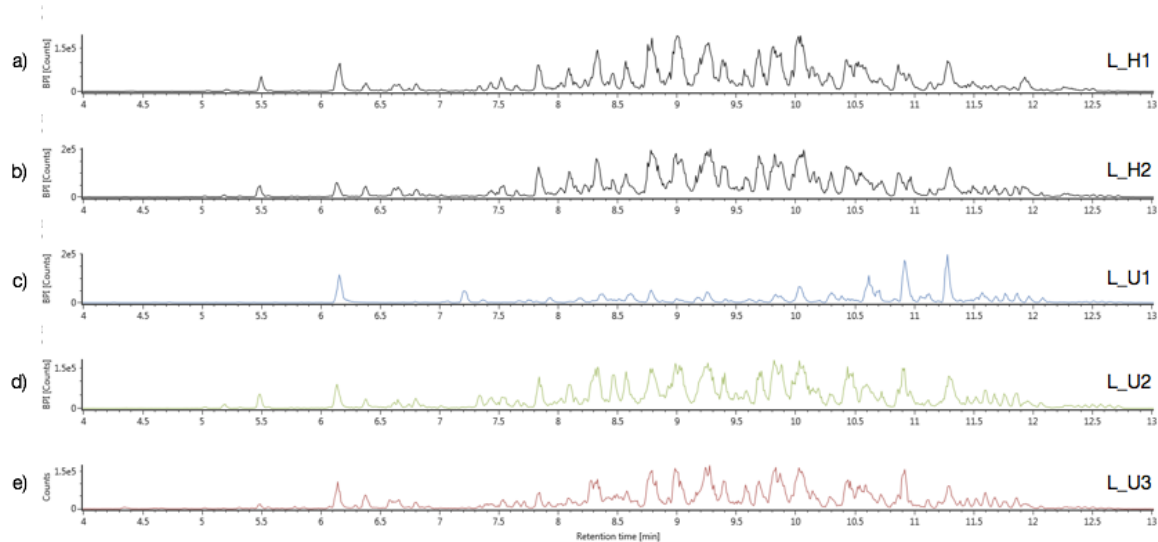


Figure 7: Graphs a-e show a section (RT 4-13 min) of the BPI chromatograms from the UHPLC-HR-MS/MS analysis of healthy (L_H1, L_H2) and unhealthy (L_U1, L_U2, L_U3) Lubomirskia sponge specimens.

Figure 8 displays the segments of the metabolic profiles of the healthy and unhealthy *Rezinkovia* specimens between RT 4-13 min. The metabolic profile of the healthy specimen, R_H1, appears similar to unhealthy specimen R_U1. Though the intensities of the peaks are different, for instance from RT ~5.4-6 min, the molecules are most likely the same due to similar fragmentation patterns (not shown), though the segment of peaks from approximately RT 11.4-11.8 min in R_U1 stands out. Many peak intensities of R_U2 differ from both R_H1 and R_U1, indicating possible disruption to normal metabolic output.

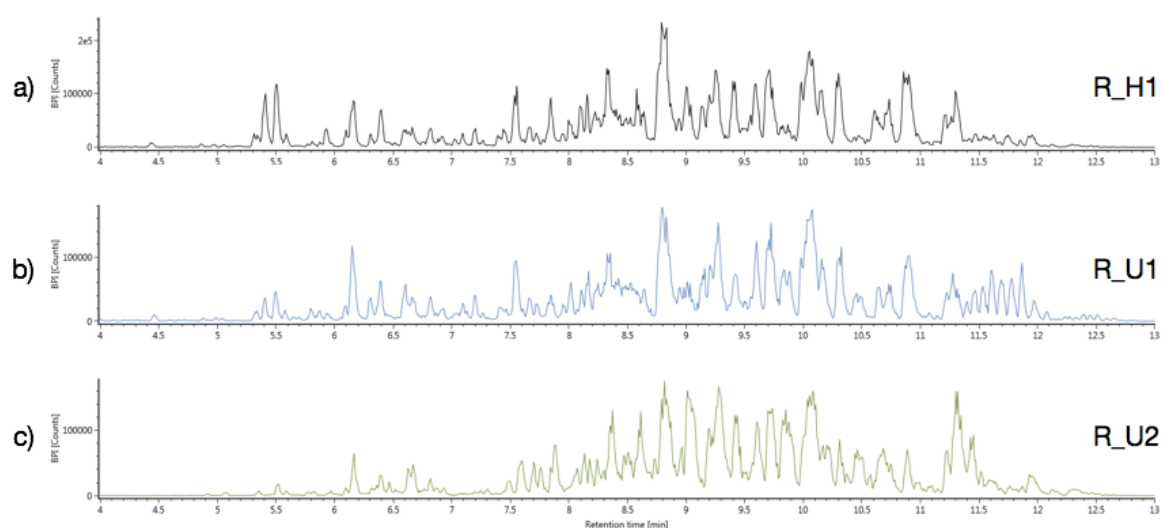


Figure 8. Graphs a-c show a section (RT 4-13 min) of the BPI chromatograms from the UHPLC-HR-MS/MS analysis of healthy (R_H1) and unhealthy (R_U1, R_U2) Rezinkovia sponge specimens.

Figure 9 shows the similarities in peak occurrence and intensity between the healthy and unhealthy *Swartschewskia* specimens. In these segments of their metabolic profiles from RT 4-13 min, S_H1 and S_U1 appear to have very similar chromatograms and relative peak intensities. The intensity of the peak at RT ~8.35 min is one exception, where the relative peak intensity is greater in S_U1.

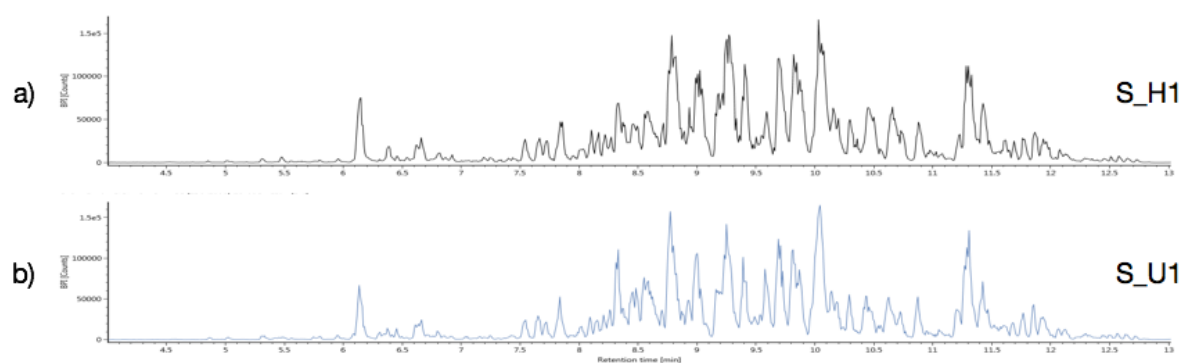


Figure 9: Graphs a and b show a section (RT 4-13 min) of the BPI chromatograms from the UHPLC-HR-MS/MS analysis of healthy (S_H1) and unhealthy (S_U1) Swartschewskia sponge specimens.

Figure 10 displays segments of the metabolic profiles of healthy and unhealthy *Baikalospongia* specimens between RT 4-13 min. There are many small differences between each of the unhealthy specimens and the healthy specimen, though in regard to the most prominent peaks, the metabolic profiles appear similar. Most notable across all specimens is the variability between the chromatogram segments from RT 5-7 min, though the peaks are relatively small in all profiles. Notably, B_U5 has the jagged peak pattern from approximately RT 11.4-11.8 min as observed in specimen R_U1, which suggests that the metabolic production of these molecules is related.

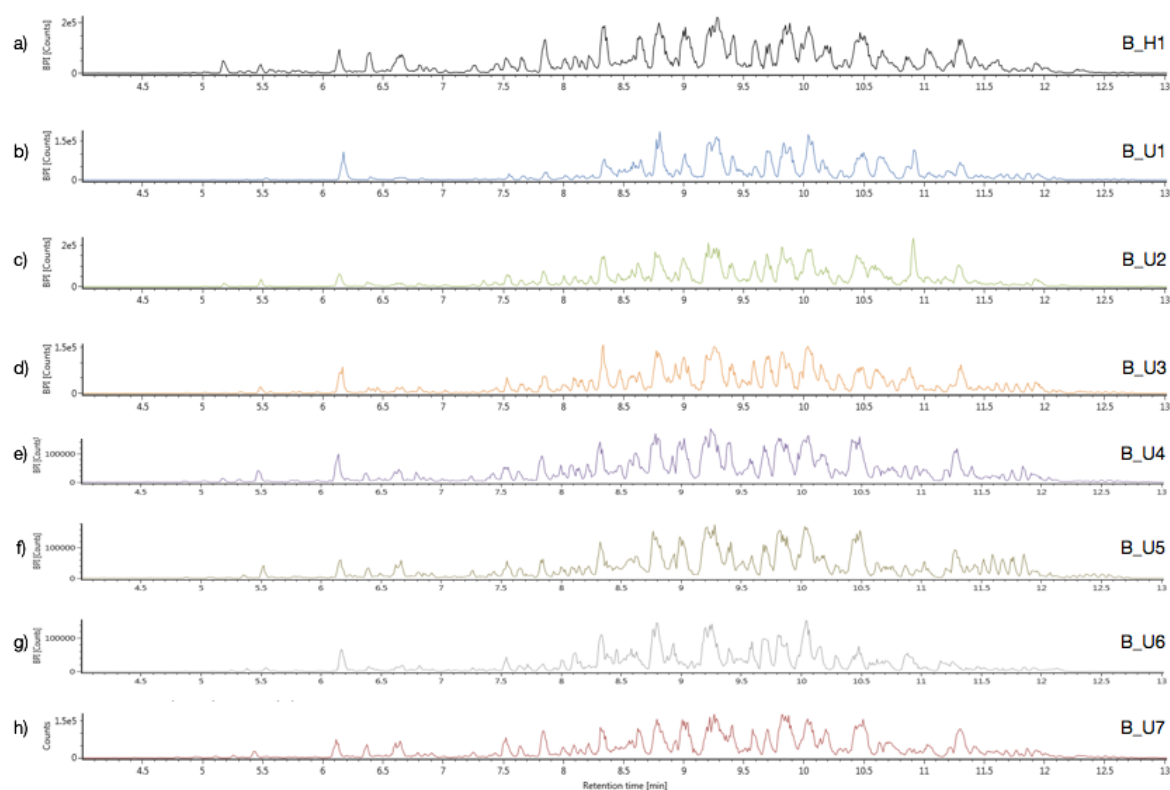


Figure 10: Graphs a-h show a section (RT 4-13 min) of the BPI chromatograms from the UHPLC-HR-MS/MS analysis of healthy (B_H1) and unhealthy (B_U1, B_U2, B_U3, B_U4, B_U5, B_U6, B_U7) *Baikalospongia* sponge specimens.

Figure 11 shows segments of the metabolic profiles of the biofilm specimens collected from the littoral zone of the Cape Tolsty sampling site in Lake Baikal between RT 4-13.5 min. When compared to both healthy and unhealthy sponge specimens, biofilm metabolic profiles generally appear different and the number of different molecules detected by the mass spectrometry system are fewer. When studying the metabolic profiles of just the biofilm specimens, BF_1 and BF_2 appear to have greater similarities in their metabolic profiles than when either is compared to BF_3, which has a comparatively distinct profile. The peaks from RT ~11.4-11.8 min in BF_3 share similar patterns to the jagged peaks seen in unhealthy *Rezinkovia* specimen R_U1.

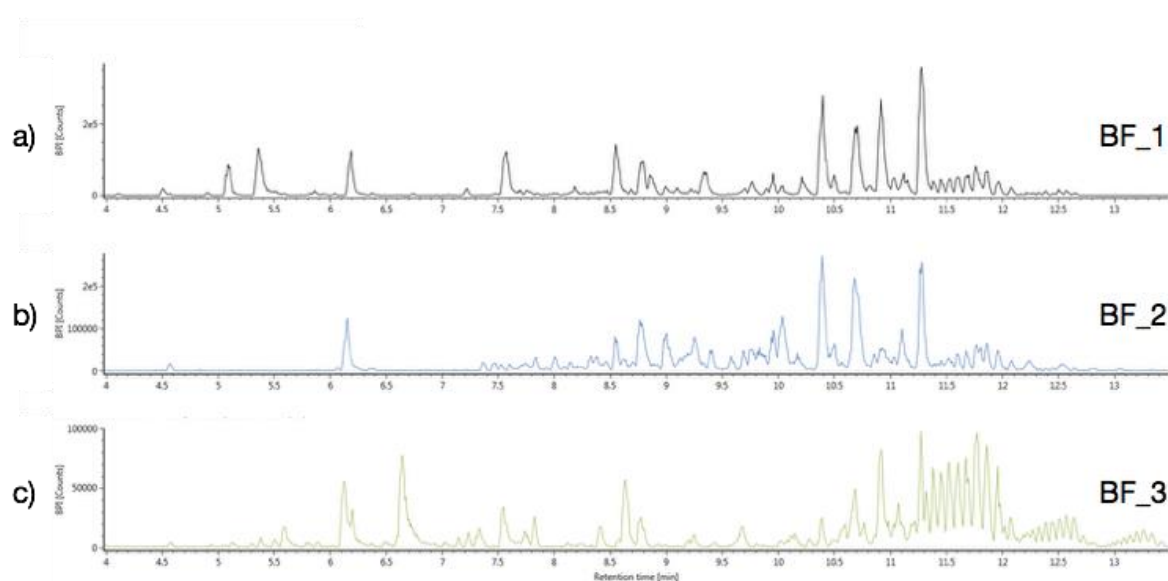


Figure 11. Graphs a-c show a section (RT 4-13.5 min) of the BPI chromatograms from the UHPLC-HR-MS/MS analysis of biofilm specimens (BF_1, BF_2, BF_3).

2.6.3 Search for Identifiable Molecules

The search for secondary metabolites produced by cyanobacteria in the healthy and unhealthy specimens had several iterations. There was an initial investigation into peaks that had relative intensities of >4.6%. Then secondary metabolites found during a literature search (Mehner et al., 2008, Kleinteich et al., 2013, Shams et al., 2015, Salmaso et al., 2016), produced by *Tychonema spp.* and *Tolypothrix distorta*, were searched for in peaks measuring >30,000 detection units. Molecule fragmentation patterns typically associated with microcystins and aeruginosins were manually searched through for these cyanotoxins in all peaks with >1 detection unit. The search for secondary metabolites produced by cyanobacteria was unsuccessful in all healthy and unhealthy sponge specimens. Similarly, the search was unsuccessful in biofilm specimens in peaks measuring >30,000 detection units. Since the maximum amount of detection units for a single peak was >10,000,000 in most specimens,

30,000 detection units included molecules that had a minimum 0.20-0.76% relative intensity, depending on the specimen. The number of molecules detected for each sponge specimen was generally >10,000, and it was not possible to manually investigate and elucidate the structure of the majority of them.

Though we were unable to find secondary metabolites produced by cyanobacteria, the metabolic profile of L_U1 warranted further investigation. Peaks with higher relative peak intensities were the focus. Molecules that had relative peak intensities >4.6% and an i-FIT confidence >99% with a molecule from the ChemSpider database were selected for comparison.

In **Table 3**, the relative peak intensities for the selected molecules are compared in all sponge samples. The molecules are identified by their probable chemical structures as the molecules had multiple identity matches from the databases, all with the same i-FIT confidence percentages (**Appendix 2: Figure 18**). The molecule with m/z (H⁺) 458.3 (RT 7.2 min) has a high relative peak intensity in L_U1 but is undetected in nearly all other specimens, with the exception of B_U3. Similarly, the molecule with m/z (H⁺) 533.2 (RT 11.1 min) has a higher relative peak intensity in L_U1 but is undetected in most other specimens. The molecule with m/z (H⁺) 501.4 (RT 8.1 min), meanwhile, is found in both healthy and unhealthy specimens from nearly all sponge genera.

Table 3: The relative peak intensities (%) of five molecules identified by their probable chemical structures, based on their similar retention times (RT), mass-to-charge ratios (m/z (H^+)), and fragmentation patterns, found in the healthy and unhealthy sponge specimens. Dashed lines indicate that the compound was not detected at the minimum of 30,000 detection units used to filter the molecules.

		Identified Molecules				
		C ₂₇ H ₅₆ N ₂ O ₃	C ₂₄ H ₄₇ N ₃ O ₅	C ₂₈ H ₅₆ N ₂ O ₅	C ₃₂ H ₅₆ O ₄	C ₃₃ H ₃₂ N ₄ O ₃
		m/z 457.4	458.3	501.4	505.4	533.2
		RT 10.5 min	7.2 min	8.1 min	7.3 min	11.1 min
<i>Lubomirskia</i>	L_H1	--	--	--	--	--
	L_H2	--	--	--	--	--
	L_U1	5.1	43.1	18.2	7.6	15.2
	L_U2	--	--	0.4	--	0.8
	L_U3	0.4	--	2.6	0.4	--
<i>Swartschewska</i>	S_H1	--	--	1.16	--	--
	S_U1	--	--	--	--	--
<i>Rezinkovia</i>	R_H1	--	--	5.6	0.6	--
	R_U1	0.7	--	8.2	0.4	--
	R_U2	--	--	1.3	0.7	--
<i>Baikalospongia</i>	B_H1	0.4	--	1.2	--	--
	B_U1	0.8	--	1.4	--	--
	B_U2	--	--	1.6	--	0.9
	B_U3	1.5	0.5	--	--	--
	B_U4	0.4	--	0.3	--	--
	B_U5	--	--	2.3	--	--
	B_U6	1.3	--	2	--	--
	B_U7	0.4	--	1.6	--	--

2.6.4 Global Natural Product Social Molecular Networking (GNPS)

In order to conduct a more high-throughput investigation using the metabolic data, molecular networks were created for the different sponge genera using GNPS. Molecules, represented by nodes, were aligned with other molecules with similar fragmentation patterns. The similarity of the aligned spectrums to one another was represented by an edge line. The majority of molecules were unidentified via the GNPS molecular databases though there were some identified lysophospholipids and glycerophospholipids (**Appendix 3: Figure 19**). Additionally, pheophorbide *a* with m/z (H^+) 593.2 was identified in all *Lubomirskia*, two

unhealthy *Baikalospongia*, and all biofilm specimens. Though most molecules were unidentified, hundreds of clusters were generated from the healthy and unhealthy samples from each genus, creating “families” of molecules and illuminating the presence of molecules with related structures within the samples. An example of a cluster containing pheophorbide a, in *Lubomirskia* specimens, can be seen in **Appendix 3: Figure 20**. The majority of families had 2-10 nodes (representing individual molecules), though there were families of molecules with up to 97 individual nodes in *Baikalospongia* specimens. *Baikalospongia* specimens had 429 molecular families, *Lubomirskia* specimens had 336 families, *Swartschewskia* specimens had 137 families, and *Rezinokvia* specimens had 217 families. Clusters did not necessarily contain molecules from all specimens from the same genus, confirming that the presence of some families of molecules (as interpreted by GNPS) differed between unhealthy and healthy specimens.

2.7 Sponge-Associated Microbial Communities

Using 16S rRNA sequencing, the bacterial metagenome of the sponge and biofilm specimens were analyzed. Illumina-sequenced data was dereplicated and filtered for obtain high quality sequence. Sequences were aligned and assigned to ASVs using the DADA2 database. Data analysis was done in R Studio 1.3.959 (R Core Team, 2018). Non-metric multidimensional scaling (NMDS) of the package *vegan* 2.5-6 (Oksanen et al., 2019) was performed on the ASVs after the removal of chloroplast ASVs. Unhealthy specimen B_U3 was not sequenced so it is absent from further analyses.

2.7.1 Differences in Phyla

A total of 29 bacterial phyla were identified in the sponge and biofilm specimens, including those that remain unclassified. Bacteria from phyla Actinobacteria, Cyanobacteria, Patescibacteria, Planctomycetes, and Proteobacteria were present in all sponge and biofilm specimens (**Figure 12**). Bacteroidetes and Verrucomicrobia were also present in almost all specimens. In *Lubomirskia*, *Rezinokvia*, and *Swartschewskia* unhealthy sponge specimens, the relative abundance of Proteobacteria increased and the relative abundance of Cyanobacteria decreased in comparison to their healthy counterparts. In comparison to B_H1, the relative abundance of Proteobacteria in unhealthy *Baikalospongia* specimens is similar, but there appears to be at least a small decrease in the relative abundance of Cyanobacteria in all specimens. The appearance of phyla with lower relative abundances, such as Acidobacteria, Dadabacteria, and Spirochaetes, appears to be random and not dependent on whether the

sponge is healthy or unhealthy. In the biofilm specimens, the relative abundances of the most abundant phyla are similar, with the exception of Cyanobacteria and Verrucomicrobia. BF_3 appears to be the most diverse biofilm specimen, containing members from 23 phyla (**Figure 12**).



Figure 12: The relative abundances of bacterial phyla in sponge and biofilm specimens. Different sponge genera and biofilm specimens are grouped together and separated with dashed lines. The healthy sponge specimens representing each genus are highlighted on the x-axis. Bubble size corresponds to relative abundance percentage (%). The different disease symptoms, detailed in Appendix 1, associated with the diseased sponges are represented above the relevant specimens, with the legend in the top right.

2.7.2 Differences in Cyanobacterial Communities

In all sponge specimens, members of Synechococcales have the greatest relative abundance of the Cyanobacteria phylum (**Figure 13a**). Members of Oscillatoriales have second greatest relative abundance in some healthy and unhealthy specimens. Additionally, it can be observed that in some *Lubomirskia* and *Baikalospongia* unhealthy samples, there is more diversity in cyanobacterial orders than in their healthy counterparts. L_U1, B_U1, B_U2, and B_U6 contain members from Oscillatoriales, Nostocales, and Vampirovibrionales, in addition to

unclassified orders. In the biofilm specimens, there is a diverse range of cyanobacterial orders present, and in BF_2 the order with greatest relative abundance is Nostocales (**Figure 13a**).

A closer look at the cyanobacterial genera in the specimens reveals the dominance of *Synechococcus* (Synechococcales, **Figure 13b**). Members of the genus *Tychonema* (Oscillatoriales) is present in both unhealthy and healthy specimens, as well as two of the biofilm specimens. They have a considerable share in the cyanobacterial communities in the specimens that they are found in. The most diverse cyanobacterial communities in the sponges are in B_U1, B_U2, and L_U1. B_U1 and L_U1 share many of the same minor genera including *Chamaesiphon*, *Phormidesmis*, and *Phormidium*. In BF_2, the cyanobacterial community is dominated by members of the *Tolypothrix* genus (Nostocales) (**Figure 13b**).

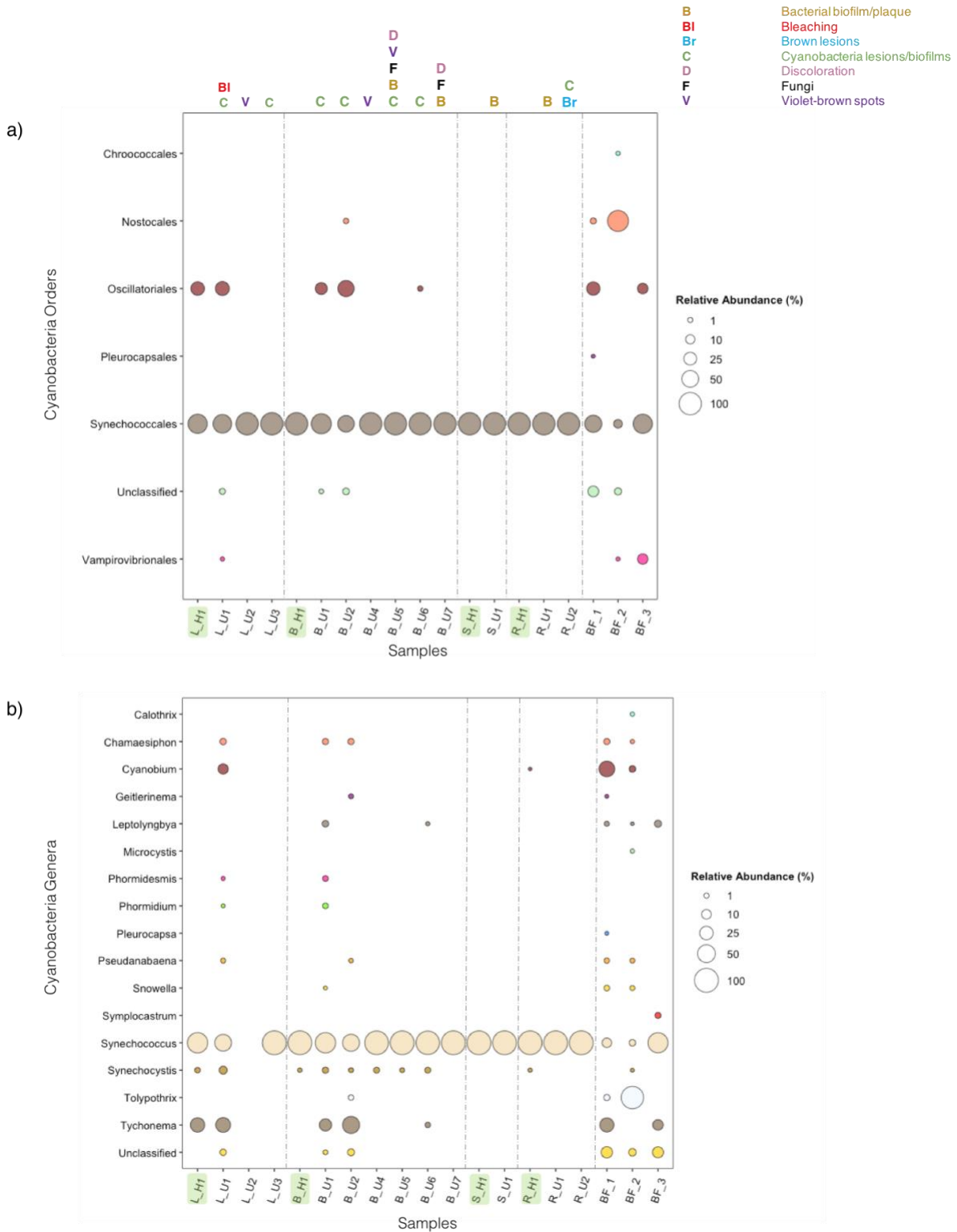


Figure 13: a) The relative abundance of cyanobacterial orders in sponge and biofilm specimens. Different sponge genera and biofilm specimens are separated by dashed lines. The healthy sponge specimens from each genus are highlighted on the x-axis. b) The relative abundance of cyanobacterial genera in sponge and biofilm specimens. Different genera and biofilm specimens are separated by dashed lines. The healthy sponge specimens representing each genus are highlighted on the x-axis. Bubble size corresponds to relative abundance percentage (%). The different disease symptoms, detailed in Appendix 1, associated with the diseased sponges are represented above the relevant specimens, with the legend in the top right.

2.7.3 Differences in Proteobacteria and Bacteroidetes Communities

Though Proteobacteria and Bacteroidetes were not the focus of our investigation, their increases in relative abundance in unhealthy specimen L_U1 were interesting enough to warrant a closer look.

Betaproteobacteriales, Rhizobiales, and Legionellales of the phylum Proteobacteria are present in all sponge and biofilm specimens (**Figure 14**) though there are variations in the microbial composition in between the healthy sponges of the four studied sponge genera. In *Lubomirskia* sponges, there is an increase in the relative abundance of Legionellales in unhealthy specimens L_U2 and L_U3. In L_U1, Rhodobacterales is the dominant order and there is higher diversity coupled with lower relative abundance of other orders. In unhealthy *Rezinkovia* sponges, there is less relative abundance of Legionellales and greater relative abundance of Rhodospirillales. In the unhealthy *Swartschewskia* specimen, Desulfarculales, Rhizobiales, and Rhodobacterales are the most dominant orders. In unhealthy *Baikalospongia* sponges, several trends can be observed. Rhodospirillales relative abundance is smaller while relative abundance of Rhizobiales and Legionellales is greater, in comparison to the B_H1.

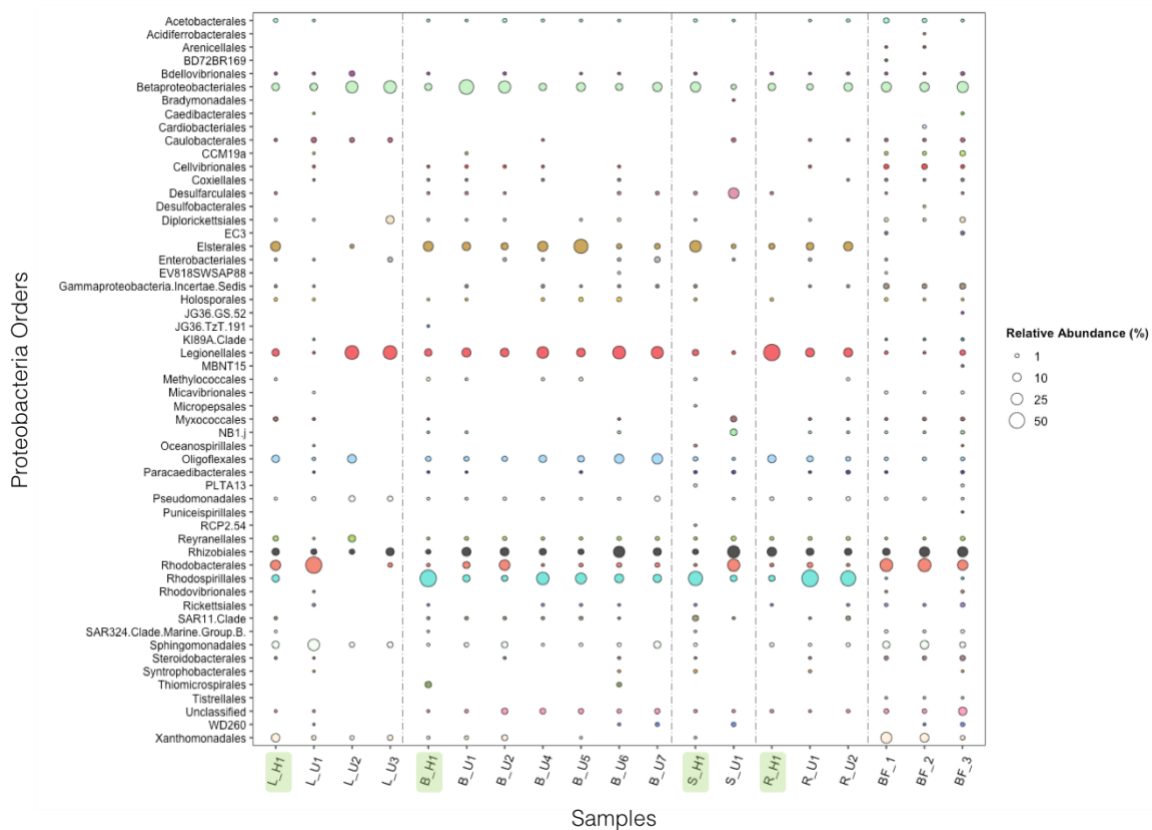


Figure 14: The relative abundance of Proteobacteria orders in sponge and biofilm specimens. Different sponge genera and biofilm specimens are separated by dashed lines. The healthy sponge specimens representing each genus are highlighted on the x-axis. Bubble size corresponds to relative abundance percentage (%).

Within the phylum Bacteroidetes, Chitinophagales is present and dominant in nearly all sponge and biofilm specimens (**Figure 15**). The exceptions are L_U2, where the phylum Bacteroidetes is absent, and B_U7, where Bacteroidales is the only one present. Flavobacteriales, Cytophagales, and Sphingobacteriales are also present in smaller amounts in a majority of the samples.

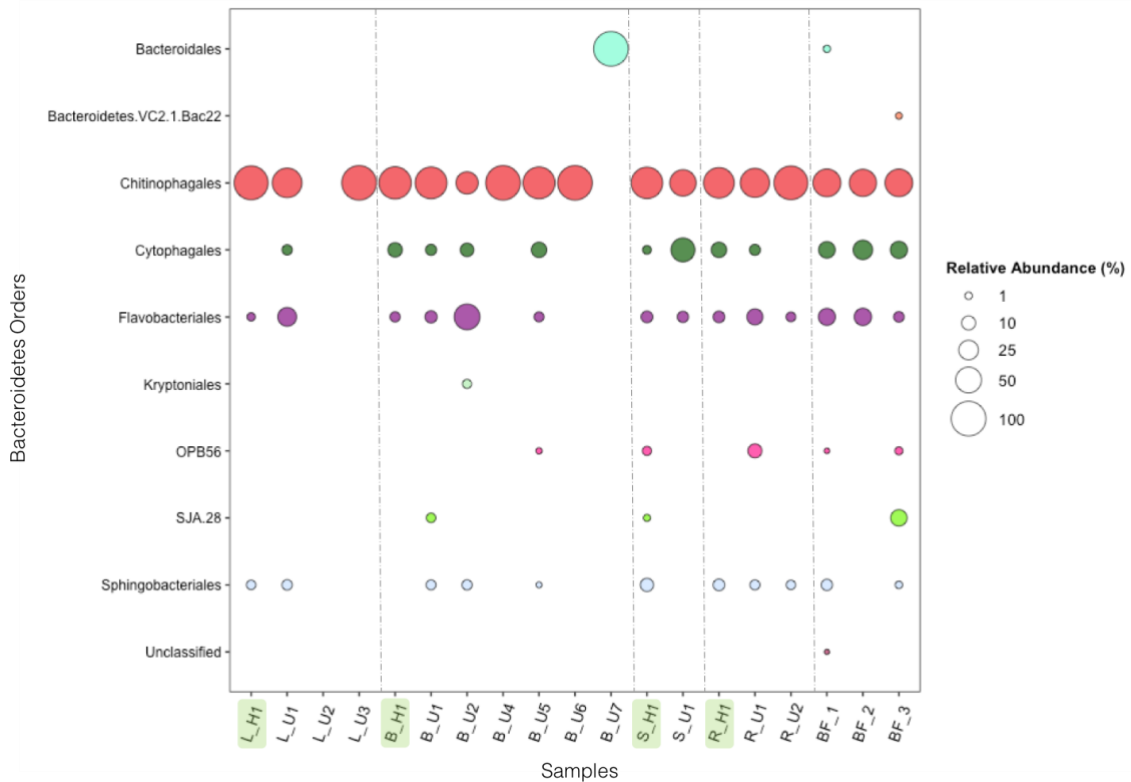


Figure 15: The relative abundance of Bacteroidetes orders in sponge and biofilm specimens. Different sponge genera and biofilm specimens are separated by dashed lines. The healthy sponge specimens representing each genus are highlighted on the x-axis. Bubble size corresponds to relative abundance percentage (%).

2.7.4 Dissimilarities at Phylum Level

ASV relative abundance data was used to generate an NMDS plot in which the closeness of microbial communities of the different sponge and biofilm specimens was compared. Biofilm samples were distributed separately from the sponge samples (**Figure 16**). Despite biofilm formation on many of the sponges, the overall microbial community structure is not affected to the point that the unhealthy sponges and biofilm communities completely resemble each other. Overall, unhealthy specimens are plotted away from their healthy counterparts, indicating a difference in microbial communities at the phylum level. Unhealthy specimens differ in their microbial community structures in relation to the healthy representatives of their respective genus, and some specimens are “more” dissimilar than others. For instance, *Baikalospongia* unhealthy specimens with discolored bodies (B_U5, B_U7) cluster together

on this plot and are two of the *Baikalospongia* specimens most dissimilar to the healthy specimen. B_U1 and B_U2, on the other hand, are less dissimilar from B_H1, and both had cyanobacterial biofilms growing on the sponge surface. While they are least dissimilar from the healthy *Baikalospongia* specimen, they also seem to cluster near L_U1, which exhibited both prominent bleaching and cyanobacterial biofilm growth.

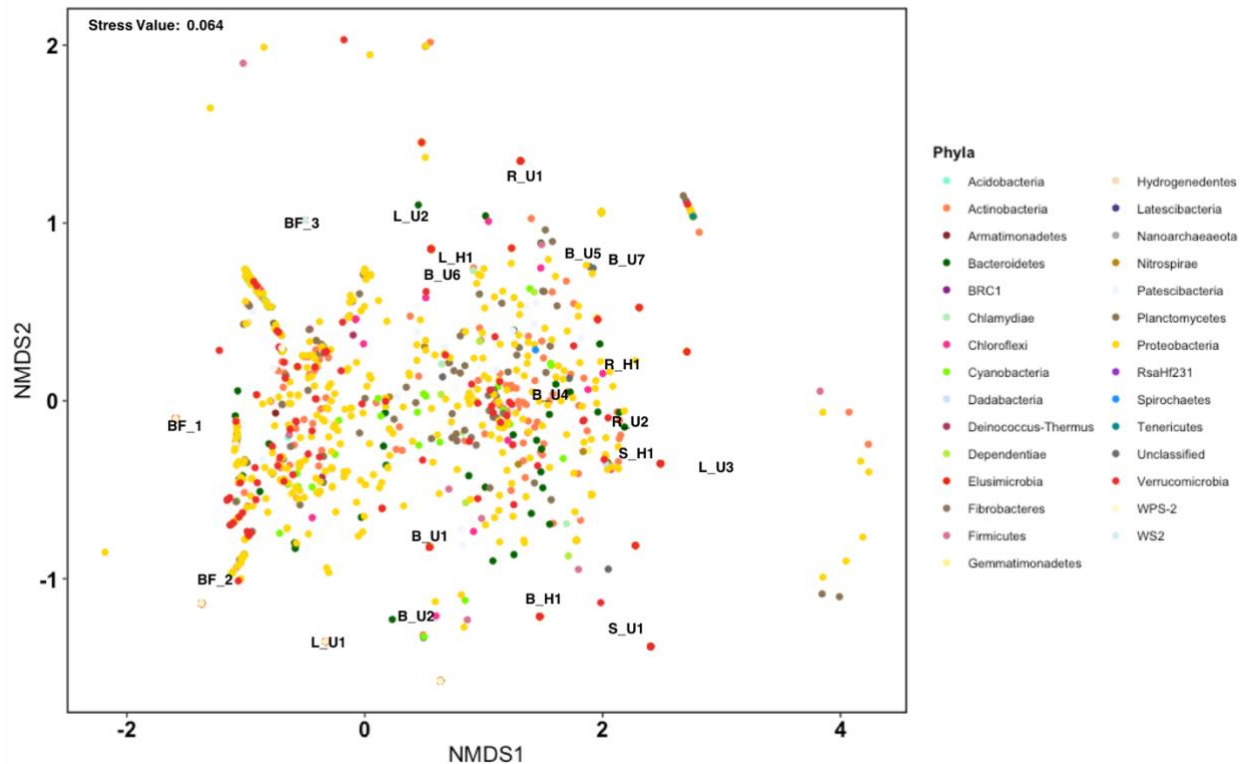


Figure 16: Non-metric multidimensional scaling (NMDS) plot of dissimilarities between healthy sponge, unhealthy sponge, and biofilm specimens. The colored dots represent individual ASVs, with their associated phylum indicated by the colors presented in the legend. The plot was generated using the Bray-Curtis dissimilarity matrix using data that underwent square root transformation and Wisconsin double standardization. The stress value indicates the goodness of fit of the model, with 0 indicating a perfect fit and <0.1 a great fit.

3 Discussion

In this thesis, we aimed to compare the metabolic profiles of healthy and diseased sponges from Lake Baikal using an untargeted metabolomics approach with UHPLC-HR-MS/MS. We expected to find and identify cyanobacterial toxins associated with the cyanobacterial species growing in biofilms on the diseased sponges, as cyanobacteria have been speculated to be the etiological agent of disease in the Lake Baikal sponges. Using bacterial metagenome sequencing data for each specimen, we aimed to compare the sequencing profiles of healthy and diseased sponges and use this information, in tandem with the metabolic profiles, to determine the role of cyanobacteria in causing sponge disease and necrosis in Lake Baikal. Though cyanobacterial-associated toxins were not found in our analysis, shifts in sponge metabolomes were observed that seemed to correlate with dysbiosis in the symbiont microbial composition.

3.1 Specimen Diversity

Lubomirskia baikalensis, *Baikalospongia bacillifera*, and *Baikalospongia intermedia* are the most abundant species in the lake (Belikov et al., 2007). In our selection of sponges, *Baikalospongia* sponges make up the majority of specimens, with the healthy replicates both from Bolshie Koty, and diseased specimens from Cape Tolsty and Bolshie Koty (**Appendix 1**). In *Lubormirskia* sponges, the specimens had similar origins, though there were fewer. Therefore the “controls” in the form of healthy specimens do not necessarily represent the intraspecific variation between metabolome and symbiont microbial communities from different localities in these genera.

3.2 Metabolic Profiling

3.2.1 Mass Spectrometry Chromatograms

Sponges are known for being prolific sources of novel natural products, though the focus has been primarily on mining them from marine environments. Comparing the chromatograms of the healthy specimens from the four genera against each other revealed that they have similar metabolic profiles (**Figure 6**). However, when relative peak intensities for randomly selected shared peaks were calculated, *Rezinkovia* differed from *Swartschewska*, *Lubormirskia*, and *Baikalospongia* in the peak which had the highest relative intensity (**Table 2**). Other differences between the relative peak intensities do not seem to follow any patterns, though the *Baikalospongia* specimen seemed to have comparatively low relative peak expression for

the few selected molecules in **Table 2**. Compared to the metabolic output of biofilm specimens (**Figure 11**), healthy sponges produced a much greater number of unique, detectable molecules, which confirms that they or their symbionts are prolific sources of natural products.

When the chromatograms of the healthy specimens and unhealthy specimens from each genus were compared to one another, samples designated as unhealthy had distinct metabolome compositions. Metabolomes of unhealthy specimens such as L_U1 (**Figure 7**) and R_U2 (**Figure 8**) differed dramatically from their healthy counterparts. For the most part, these specimens exhibited a dramatic decrease in the diversity of their metabolic production. However, certain metabolites were significantly elevated in L_U1, constituting a larger relative peak intensity of the metabolome than any other unhealthy or healthy specimen from all four investigated sponge genera (**Table 3**). The chromatograms for L_U1 and R_U2 indicate that it is likely that differences between their microbial communities influenced their metabolic output.

In *Swartschewskia*, the chromatograms and relative peak intensities of the metabolomes of the healthy and unhealthy specimens were almost identical, despite a bacterial biofilm being noted on the unhealthy sample (**Figure 9**). In *Lubomirskia*, unhealthy specimens with cyanobacterial spots had metabolic profiles with greater similarities to their healthy counterpart, rather than bleached specimen L_U1 (**Figure 7**). Similarly, in *Rezinkovia*, the metabolomic profile of the unhealthy specimen noted to have a bacterial plaque resembled the healthy specimen more than R_U2, which had noticeable brown spots and diatom algae (**Figure 8**). Within the *Baikalospongia* genus, which included the largest number of unhealthy specimens, the metabolomic profiles of the specimens identified as having large cyanobacterial biofilms had the most noticeable differences from the healthy specimen. A flat species of *Baikalospongia*, noted as growing amongst cyanobacterial and diatom biofilms, also seemed to have a distinct metabolomic profile compared to the healthy specimen (**Figure 10**). The latter variation is likely influenced by interspecific differences between *Baikalospongia* species (Reverter et al., 2018). Across all genera, the visibly unhealthy sponges with “extreme” manifestations of disease (e.g. bleaching, brown spots, large cyanobacterial biofilms) seem to have distinctly different metabolomic profiles than visibly unhealthy sponges with “less extreme” manifestations of disease (e.g. small violet-brown spots, bacterial plaques), when compared to the respective healthy specimens.

In marine environments, the variability of sponge metabolomes has been attributed to a variety of factors. These include local environmental and temporal changes, such as increasing temperatures (Reverter et al., 2016) and a response to shifting seasons (Ternon et al., 2017), as well as competitive interactions with other invertebrates (De Caralt et al., 2013) and reproductive periods (Reverter et al., 2018). In freshwater environments, the same influences most likely apply. The metabolomes of the Lubomirskiidae sponges in Lake Baikal are overall similar due to environmental and seasonal factors but have variations intergenera, which are most likely due to differences in the holobiont composition. Reverter et al., 2018 note the greater influence of interspecific, rather than intraspecific, variation on the metabolomes of the marine *Haliclona* sponge species.

3.2.2 Search for Cyanobacterial Natural Products

Known secondary metabolites produced by *Tychonema bourrellyi* and *Tolypothrix distorta*, such as tychonamide a and b (Mehner et al., 2008), anatoxin-a (Shams et al., 2015), homoanatoxin-a (Salmaso et al., 2016), using the m/z and fragmentation spectrums in the literature, were searched for in all specimens. Saxitoxin, previously detected during a cyanobacterial bloom, was searched for using the known m/z and fragmentation spectrum (Grachev et al., 2018). Characteristic fragment ions for microcystins and aeruginosins were used as the basis for a thorough search through the different molecules detected in all healthy and unhealthy specimens (Caixach et al., 2016), though no such ions were ultimately found. The cyanotoxins hypothesized to be produced by the cyanobacterial species previously found on sponge specimens (Sorokovikova et al., 2020) and in cyanobacterial blooms (Grachev et al., 2018) in Lake Baikal were not found in our investigation. The cyanobacterial natural products found in the aforementioned studies are therefore most likely not the causes of the different disease manifestations in Lake Baikal sponges.

3.2.3 Global Natural Product Social Molecular Networking

Several molecules were identified via GNPS molecular networking, the majority of them lysophospholipids (LPLs) (**Appendix 3: Figure 19**). LPLs were also tentatively identified, though their identities were not able to be confirmed, in our manual search through peaks in the specimen chromatograms. A closer investigation into the fragmentation patterns of the prominent peaks in the sponge chromatograms confirmed the presence of a fragment ion with m/z 184, likely phosphocholine, which is characteristic of LPLs (Murph et al., 2007). Clusters consisting of identified LPLs and unidentified derivative molecules were seen in all four

genera, confirming the ubiquitous and widespread nature of LPLs in *Lubomirskiidae* sponges. Differences in metabolic patterns, through presence or absence of the GNPS identified molecules, confirmed that production of LPLs changes between healthy and diseased sponge specimens of the same genus. For instance, LPC (17:0/0:0) with chemical structure $C_{25}H_{52}NO_7P$, was identified in all specimens from *Lubomirskia* with the exception of L_U1.

Lipids, including fatty acids, phospholipids, and sterols, are integral sponge metabolites. LPLs, which include platelet-activating factor (PAF) and glycerophospholipid metabolic pathway intermediate phosphocholine, are widely distributed molecules in invertebrate animals (Sugiura et al., 1992) and have been documented in a variety of sponge species, including sponges from the *Lubomirskiidae* family (Latyshev et al., 1992, Dembitsky et al., 1993, Imbs & Latyshev, 1998, Dembitsky et al., 2003). Fatty acids and lipids isolated from marine and freshwater sponges differ, and Demospongiae in particular are known for their very long-chain fatty acids (C₂₄-C₃₈) (Dembitsky et al., 1993, Bergquist et al., 1984, Dembitsky et al., 2003). LPLs, a subgroup of the glycerophospholipid class of lipids, differs from phospholipids in their lack of one of their fatty acyl chains (Murph et al., 2007). Despite their ubiquitous nature, the role of LPLs in invertebrate physiology is yet to be determined. Invertebrate defense seems to be the prevailing theory (Reverter et al., 2018), though there is also evidence for their involvement in several reproductive stages (Ivanisevic et al., 2011).

Reverter et al., 2018 point out that in accordance with the optimal defense theory proposed by Rhoades 1985 for plant and herbivore interactions, the production of secondary metabolites hinges on the reallocation of energy used for primary functions and vice versa. This trade-off is seen in marine sponges, where metabolic production decreases during energy demanding reproduction and growth stages (López-Legentil et al., 2006). Therefore, it can be assumed that during the invasion of opportunistic pathogens, energy is directed towards defense i.e. the production of cytotoxic and antibacterial/antifungal metabolites. However, it should be noted that this may not be applicable in all sponge species.

Other than LPLs, pheophorbide *a* was identified using GNPS molecular networking. A related molecule tentatively identified as chlorophyllone *a* was later found in a manual search of the chromatogram peaks in specimen L_U1. Chlorophyllone *a* and pheophorbide *a* are both products in the multi-step so-called PAO pathway of chlorophyll *a* degradation (Hörtensteiner & Kräutler, 2011). Colorless catabolites are characteristic of chlorophyll degradation, which explains the disappearance of the green pigment and bleaching effect in

specimen L_U1 and discoloration in B_U5 and B_U7 (**Appendix 1**). Previously documented symbionts of Lake Baikal sponges include aforementioned dinoflagellate species and cyanobacteria, which are both chlorophyll sources for the presumed degradation products chlorophyllone *a* and pheophorbide *a*. Though in most unhealthy specimens the relative abundance of cyanobacteria is lower than in the respective healthy specimens (**Figure 12**), the amounts of pheophorbide *a* detected did not always correspond to a decrease in cyanobacterial relative abundance (calculations not shown). The degradation products are therefore assumed to result primarily from the loss of the primary dinoflagellate symbiont. Pheophorbide *a* was also found in healthy *Lubomirskia* specimens, L_H1 and L_H2. Though the relative peak intensity is low, this can be an indicator that this sponge was in the early stages of decline, despite being visibly healthy. Coral bleaching, for instance, was only visible without the use of microscopy when the majority (>50%) of its symbiont dinoflagellate community disappeared (Fitt et al., 2000). Low levels of pheophorbide *a* were also found in the biofilm specimens via GNPS molecular networking, indicating chlorophyll degradation.

3.2.4 Untargeted Metabolomics Limitations

High peak intensity does not necessarily mean high molecular bioactivity. LPLs are easily ionized molecules, which translates to prominent chromatogram peaks. As the number of molecules detected in each specimen was incredibly high, and there was only so much time available to investigate the fragmentation patterns of individual peaks, the prominence of LPLs can distract from less prominent peaks with more bioactivity. We also noticed that many peaks had low i-FIT confidence and remained unidentified by the ChemSpider database. An incomplete database of freshwater natural products may explain the lack of identifiable natural products. There is a documented bias for molecules extracted from marine cyanobacteria and the mining of natural products has been focused on marine invertebrates (Tidgewell et al., 2010). Though freshwater sponges compose a small fraction of the thousands of known sponge species, they are reservoirs of unusual fatty acids and lipids (Dembitsky et al., 2003). Since molecular products made by free-living bacteria differ structurally from those made by bacteria in symbiosis (Kampa et al., 2013), it is crucial to capture the full diversity of microbial natural products, from all environments ranging from marine to freshwater to terrestrial, in accessible databases. In addition to Cyanobacteria, there are also untapped sources of secondary metabolites, from phyla Acidobacteria, Gemmatimonadetes, Verrucomicrobia, and candidate phylum Rokubacteria, which have NRPS and PKS biosynthetic gene clusters (Crits-Cristoph et al., 2018).

3.3 Metagenomic Profiling

3.3.1 Changes in Microbial Community Structure

The lack of identifiable cyanobacterial secondary metabolites prompted us to investigate the microbial community structures of the specimens. Overall, diseased specimens experienced a reduction in the relative abundance of cyanobacteria (**Figure 12**). In *Lubomirskia* unhealthy specimen L_U3 cyanobacterial ASVs are nearly absent, though the metabolic output of L_U3 and the healthy specimen appear similar (**Figure 7, Figure 12**). The dominant cyanobacterial genus in both healthy and unhealthy samples is *Synechococcus*, corroborating the findings in Sorokovikova et al., (2020). Also, in accordance with their observations, members of the *Tychonema* genus were present in some diseased specimens and dominant community members in lesions (**Figure 13, Appendix 4**). Unexpectedly, *Tychonema* made up a significant portion of the cyanobacterial community in the healthy *Lubomirskia* representative. This, along with the absence of cyanobacterial lesions from other specimens without *Tychonema*, indicates that *Tychonema* alone is not responsible for this particular disease manifestation. Earlier studies noted a dominance of *Synechococcus* and lower cyanobacterial diversity in diseased specimens (Kaluzhnaya & Itskovich, 2015, Denikina et al., 2016). Our findings indicate a different trend in unhealthy specimens: one of increased cyanobacterial diversity and lower relative abundances of *Synechococcus* members in diseased specimens.

3.3.2 Decrease in Symbiont Cyanobacteria

As proposed by Khanaev et al., (2017) and Kulakova et al., (2018), our findings suggest that cyanobacterial biofilms are most likely formed on the sponges by opportunistic cyanobacteria, due to dysbiosis in the sponge's microbial communities. In fact, symbiont cyanobacterial communities seem to be suffering from the effects of dysbiosis more than members of other phyla. The majority of diseased specimens lack cyanobacteria notorious for secondary metabolite production (**Figure 13**). This, for the most part, explains why we were unable to find cyanobacterial toxins in the metabolic analysis of our specimens. The production of cyanotoxins may be more localized to lesion sites on the surface of the sponge. There was evidence that the relative abundance of cyanobacterial communities at lesion sites may be greater than what is found in the entire sponge body (**Appendix 4**). In relation to our metabolic data, as our lyophilized specimens included the entire sponge body, smaller, but still bioactive, peaks may have been obscured.

This decrease in cyanobacteria symbionts is curious. One of the changes observed in tandem with the appearance of diseased sponges in Lake Baikal has been the appearance of *Spirogyra* algal blooms (Timoshkin et al., 2016). This unusual growth of *Spirogyra* has been linked to groundwater contamination from untreated human waste. *Spirogyra* has observed allelopathic effects on the growth of cyanobacteria *Microcystis aeruginosa* (Chroococcales). After an initial period of stimulated growth during exposure to *Spirogyra* macrophytes, pure *M. aeruginosa* cultures experienced growth inhibition and lower chlorophyll *a* levels (Liu et al., 2019). Though this allelopathic inhibition effect may not be the same for other cyanobacterial species, particularly symbionts of *Lubomirskiidae* sponges, it may be something to consider. In addition to the sponge and biofilm specimens collected for our study, a couple of biofilms of eukaryotic (e.g. *Spirogyra*) origin were collected from the littoral zone of Listvyanka (**Figure 3**), which is a separate location from where the sponge and bacterial biofilm specimens were collected. Cape Tolsty and Bolshie Koty were noted as places where the presence of *Spirogyra* was, respectively, unknown and found sporadically (Timoshkin et al., 2016).

3.3.3 Similar Trends in Proteobacteria and Bacteroidetes Phyla

Though our focus was on the phylum Cyanobacteria, other phyla experienced changes that are notable. Sequencing results show that diseased specimens have different microbial communities from counterpart healthy species, and that even the healthy sponges vary between genera in their microbial community composition (**Figure 16**). The most dramatic difference in sponge microbial community composition, from its healthy counterpart, occurred in *Lubomirskia* specimen L_U1 (**Figure 12**). In comparison to bleached *Lubomirskia* sponges studied by Kaluzhnaya and Itskovich in 2015, Cyanobacteria and Actinobacteria had smaller shares in the microbiome. Proteobacteria, however, remained the dominant phylum. This is similar to observations in Great Barrier Reef coral species *Acropora hyacinthus* affected by white syndrome, i.e. bleaching (Pollock et al., 2016). A four-fold increase of members of *Rhodobacteraceae* was found in white syndrome-associated lesions, in comparison to surrounding unaffected tissue and healthy specimens. The authors speculate that these members of *Rhodobacteraceae* take on the role of opportunistic pathogens in corals, due to their specific presence in highly defined diseased spots. In the majority of the diseased specimens in our study, the relative abundances of Proteobacteria did not fluctuate wildly, though the make-up of the communities on the order level deviated from the healthy specimens, differing by sponge genus (**Figure 14**). In most specimens,

Bacteroidetes had similarly stable relative abundances and microbial composition at different taxonomic levels. In L_U1, however, the relative abundance significantly increased. Another exception was, notably, L_U2 in which Bacteroidetes was totally absent, versus 1.75% in the healthy specimen (**Figure 12**). Also, when looking at order level, specimen B_U7, where Bacteroidales was the only order present, stood out from the other specimens (**Figure 15**). Members of Bacteroidetes are known for their competitive, scavenging behavior, which is associated with their ancestrally acquired ability to degrade complex, organic molecules (Munoz et al., 2020) so it is unsurprising to see them flourish in L_U1. In this particular specimen, it seems that members of Proteobacteria and Bacteroidetes are taking advantage of the dysbiosis in the sponge communities, which is giving them a competitive growth advantage over normal sponge symbionts.

3.3.4 Non-microbial Disease Etiology

Considering previous instances of non-microbial pathogens in corals and sponges, and the presence of fungal biofilms on diseased sponge surfaces (**Appendix 1**), other pathogen sources should be investigated. Corals suffering from Dark Spot Syndrome (DSS), which causes disease symptoms that appear similar to those in *Rezinkovia* specimen R_U2, were dominated by a fungus related to *Rhytisma acerinum*, which causes tar spot in trees (Sweet et al., 2013). The lack of clear prokaryotic pathogenic agents in Lake Baikal sponges highlights the need to identify eukaryotic symbionts and disruptions to normal symbiotic relationships.

4 Conclusion and Outlook

In this study we showed that metabolomes of healthy sponges differ from those of diseased sponges. The metabolome of the bleached sponge was obviously affected, with normal metabolic output essentially ceasing and accompanied by the rise of chlorophyll degradation products, which can be considered biomarkers of disease. As cyanobacteria are notorious producers of metabolites that act as toxins to eukaryotic cells, we expected to find prevalent cyanotoxins in our mass spectrometry analysis of the sponges with cyanobacterial biofilms and spots, which was not confirmed. The combined results from our mass spectrometry analysis and 16S rRNA analysis suggest that cyanobacteria are not the cause of the different manifestations of disease that are seen in Lake Baikal sponges. Our findings further support the theory that dysbiosis in Lake Baikal sponge symbiont microorganismal communities is triggered by a thus far unknown source, which is in fact causing changes in the sponge metabolome and a spectrum of physical disease manifestations. Metabolic patterns and community composition of associated symbionts in both corals and sponges have been found to deviate from the normal due to local environmental stress such as eutrophication, as well as climate change related stress, such as rising temperatures, which may be the case for Lake Baikal sponges.

The amount of information provided by studies implementing untargeted metabolomics can be enormous and we did not have time to conduct an in-depth analysis during the time allotted for this thesis. Therefore, the metabolomic data we acquired can be used to elucidate further information about the sponges and biofilms in this study. The identities of molecules can be confirmed and their bioactivities and involvement in biosynthetic pathways can be investigated. GNPS can be used to identify related molecules in biosynthetic pathways. In future studies, the design should include the study of the accumulation of metabolites in different zones in sponges and metabolic impact at lesion sites. Furthermore, based on the results of this study, comparative temporal metabolic studies are recommended for Lake Baikal sponges. Understanding the baseline of seasonal changes in their metabolomes is crucial to understanding their adaptability and stress responses to local changes from eutrophication and wider sweeping climate-related changes. Considering the vastness of the lake ecosystem and different variants of sponges, including those in deep-water hydrothermal vents, this is a big, but valuable, undertaking.

5 References

- Angermeier, H., Glöckner, V., Pawlik, J. R., Lindquist, N. L., & Hentschel, U. (2012). Sponge white patch disease affecting the Caribbean sponge *Amphimedon compressa*. *Diseases of Aquatic Organisms*, 99(2), 95-102. doi:10.3354/dao02460
- Annenkova, N. V., Lavrov, D. V., & Belikov, S. I. (2011). Dinoflagellates associated with freshwater sponges from the ancient Lake Baikal. *Protist*, 162(2), 222-236. doi:10.1016/j.protis.2010.07.002
- Beeton, A. M. (1984). The world's great lakes. *Journal of Great Lakes Research*, 10(2), 106-113. doi:10.1016/s0380-1330(84)71817-x
- Belikov, S. I., Kaluzhnaya, O. V., Schröder, H. C., Müller, I. M., & Müller, W. E. G. (2007). Lake Baikal endemic sponge *Lubormiskia baikalensis*: structure and organization of the gene family of silicatein and its role in morphogenesis. In M.R. Custódio (Ed.), *Porifera Research: Biodiversity, Innovation, and Sustainability* (pp. 179-188). Museu Nacional.
- Belikov, S. I., Feranchuk, S. I., Butina, T. V., Chernogor, L. I., Khanaev, I. V., & Maikova, O. O. (2018). Mass disease and mortality of Baikal sponges. *Limnology and Freshwater Biology*, (1), 36-42. doi:10.31951/2658-3518-2018-a-1-36
- Belikov, S., Belkova, N., Butina, T., Chernogor, L., Kley, A. M., Nalian, A., Rorex, C., Khanaev, I., Maikova, O., & Feranchuk, S. (2019). Diversity and shifts of the bacterial community associated with Baikal sponge mass mortalities. *Plos One*, 14(3). doi:10.1371/journal.pone.0213926
- Bell, J. J., Davy, S. K., Jones, T., Taylor, M. W., & Webster, N. S. (2013). Could some coral reefs become sponge reefs as our climate changes? *Global Change Biology*, 19(9), 2613-2624. doi:10.1111/gcb.12212
- Belykh, O. I., Gladkikh, A. S., Sorokovikova, E. G., Tikhonova, I. V., Potapov, S. A., & Butina, T. V. (2015). Saxitoxin-producing cyanobacteria in Lake Baikal. *Contemporary Problems of Ecology*, 8(2), 186-192. doi:10.1134/s199542551502002x
- Belykh, O. I., Fedorova, G. A., Kuzmin, A. V., Tikhonova, I. V., Timoshkin, O. A., & Sorokovikova, E. G. (2017). Microcystins in cyanobacterial biofilms from the littoral zone of Lake Baikal. *Moscow University Biological Sciences Bulletin*, 72(4), 225-231. doi:10.3103/s0096392517040022
- Bergquist, P. R., Lawson, M. P., Lavis, A., & Cambie, R. C. (1984). Fatty acid composition and the classification of the Porifera. *Biochemical Systematics and Ecology*, 12(1), 63-84. doi:10.1016/0305-1978(84)90012-7
- Blunt, J. W., Copp, B. R., Munro, M. H., Northcote, P. T., & Prinsep, M. R. (2011). Marine natural products. *Natural Product Reports*, 28(2), 196-268. doi:10.1039/c005001f
- Blunt, J. W., Carroll, A. R., Copp, B. R., Davis, R. A., Keyzers, R. A., & Prinsep, M. R. (2018). Marine natural products. *Natural Product Reports*, 35(1), 8-53. doi:10.1039/c7np00052a

- Böhm, M., Hentschel, U., Friedrich, A. B., Fieseler, L., Steffen, R., Gamulin, V., Müller, I. M., & Müller, W. E. G. (2001). Molecular response of the sponge *Suberites domuncula* to bacterial infection. *Marine Biology*, *139*(6), 1037-1045. doi:10.1007/s002270100656
- Butler, M. J., Hunt, J. H., Herrnkind, W. F., Childress, M. J., Bertelsen, R., Sharp, W., Matthews, T., Field, J. M., & Marshall, H. G. (1995). Cascading disturbances in Florida Bay, USA: Cyanobacteria blooms, sponge mortality, and implications for juvenile spiny lobsters *Panulirus argus*. *Marine Ecology Progress Series*, *129*, 119-125. doi:10.3354/meps129119
- Bychkov, I., Gagarinova, O., Orlova, I., & Bogdanov, V. (2018). Water protection zoning as an instrument of preservation for Lake Baikal. *Water*, *10*(10), 1474. doi:10.3390/w10101474
- Caixach, J., Flores, C., Spooof, L., Meriluoto, J., Schmidt, W., Mazur-Marzec, H., Hiskia, A., Kaloudis, T., & Furey, A. (2016). Liquid chromatography—mass spectrometry. In J. Meriluoto, L. Spooof, & G. A. Codd (Eds.), *Handbook of Cyanobacterial Monitoring and Cyanotoxin Analysis* (pp. 218-257). John Wiley & Sons, Ltd. doi:10.1002/9781119068761
- Callahan, B., McMurdie, P. J., Rosen, M. J., Han, A. W., Johnson, A. J. A., & Holmes, S. P. (2016). DADA2: High-resolution sample inference from Illumina amplicon data. *Nature Methods*, *13*, 581–583. <https://doi.org/10.1038/nmeth.38692>
- Carmichael, W. W. (1992). Cyanobacteria secondary metabolites—the cyanotoxins. *Journal of Applied Bacteriology*, *72*(6), 445-459. doi:10.1111/j.1365-2672.1992.tb01858.x
- Carmichael, W. W., Evans, W. R., Yin, Q. Q., Bell, P., & Moczydlowski, E. (1997). Evidence for paralytic shellfish poisons in the freshwater cyanobacterium *Lyngbya wollei* (Farlow ex Gomont) comb. nov. *Applied and Environmental Microbiology*, *63*(8), 3104-3110. doi:10.1128/aem.63.8.3104-3110.1997
- Casero, M. C., Velázquez, D., Medina-Cobo, M., Quesada, A., & Cirés, S. (2019). Unmasking the identity of toxigenic cyanobacteria driving a multi-toxin bloom by high-throughput sequencing of cyanotoxins genes and 16S rRNA metabarcoding. *Science of The Total Environment*, *665*, 367-378. doi:10.1016/j.scitotenv.2019.02.083
- Castenholz, R. W., Wilmotte, A., Herdman, M., Rippka, R., Waterbury, J. B., Iteman, I., & Hoffmann, L. (2001). Phylum BX. Cyanobacteria. In D. R. Boone, R. W. Castenholz, & G. M. Garrity (Eds.), *Bergey's Manual® of Systematic Bacteriology: Volume One : The Archaea and the Deeply Branching and Phototrophic Bacteria* (pp. 473-599). Springer New York. doi:10.1007/978-0-387-21609-6_27
- Cebrian, E., Jesus Uriz, M., Garrabou, J., & Ballesteros, E. (2011). Sponge mass mortalities in a warming Mediterranean Sea: Are Cyanobacteria-harboring species worse off? *PLoS ONE*, *6*(6). doi:10.1371/journal.pone.0020211
- Chernogor, L., Denikina, N., Kondratov, I., Solovarov, I., Khanaev, I., Belikov, S., & Ehrlich, H. (2013). Isolation and identification of the microalgal symbiont from primmorphs of the endemic freshwater sponge *Lubomirskia baicalensis* (Lubomirskiidae, Porifera). *European Journal of Phycology*, *48*(4), 497-508. doi:10.1080/09670262.2013.862306

- Crits-Christoph, A., Diamond, S., Butterfield, C. N., Thomas, B. C., & Banfield, J. F. (2018). Novel soil bacteria possess diverse genes for secondary metabolite biosynthesis. *Nature*, 558(7710), 440-444. doi:10.1038/s41586-018-0207-y
- De Caralt, S., Bry, D., Bontemps, N., Turon, X., Uriz, M., & Banaigs, B. (2013). Sources of secondary metabolite variation in *Dysidea avara* (Porifera: Demospongiae): The importance of having good neighbors. *Marine Drugs*, 11(12), 489-503. doi:10.3390/md11020489
- Dembitsky, V. M., Rezanka, T., & Kashin, A. G. (1993). Comparative study of the endemic freshwater fauna of Lake Baikal—II. Unusual lipid composition of two sponge species *Baicalospongia bacillifera* and *Baicalospongia intermedia* (Family Lubomirskiidae, Class Demospongiae). *Comparative Biochemistry and Physiology Part B: Comparative Biochemistry*, 106(4), 825-831. doi:10.1016/0305-0491(93)90037-6
- Dembitsky, V. M., Rezanka, T., & Srebnik, M. (2003). Lipid compounds of freshwater sponges: Family Spongillidae, class Demospongiae. *Chemistry and Physics of Lipids*, 123(2), 117-155. doi:10.1016/s0009-3084(03)00020-3
- Denikina, N. N., Dzyuba, E. V., Bel’Kova, N. L., Khanaev, I. V., Feranchuk, S. I., Makarov, M. M., Granin, N.G., & Belikov, S. I. (2016). The first case of disease of the sponge *Lubomirskia baicalensis*: Investigation of its microbiome. *Biology Bulletin*, 43(3), 263-270. doi:10.1134/s106235901603002x
- Diaz, M. C., & Ward, B. B. (1997). Sponge-mediated nitrification in tropical benthic communities. *Marine Ecology Progress Series*, 156, 97-107. doi:10.3354/meps156097
- Dunlap, M., & Pawlik, J. R. (1998). Spongivory by parrotfish in Florida mangrove and reef habitats. *Marine Ecology*, 19(4), 325-337. doi:10.1111/j.1439-0485.1998.tb00471.x
- Ehrenreich, I. M., Waterbury, J. B., & Webb, E. A. (2005). Distribution and diversity of natural product genes in marine and freshwater Cyanobacterial cultures and genomes. *Applied and Environmental Microbiology*, 71(11), 7401-7413. doi:10.1128/aem.71.11.7401-7413.2005
- Fitt, W. K., Mcfarland, F. K., Warner, M. E., & Chilcoat, G. C. (2000). Seasonal patterns of tissue biomass and densities of symbiotic dinoflagellates in reef corals and relation to coral bleaching. *Limnology and Oceanography*, 45(3), 677-685. doi:10.4319/lo.2000.45.3.0677
- Frank, A. M., Bandeira, N., Shen, Z., Tanner, S., Briggs, S. P., Smith, R. D., & Pevzner, P. A. (2008). Clustering millions of tandem mass spectra. *Journal of Proteome Research*, 7(1), 113-122. doi:10.1021/pr070361e
- Furrow, F. B., Amsler, C. D., McClintock, J. B., & Baker, B. J. (2003). Surface sequestration of chemical feeding deterrents in the Antarctic sponge *Latrunculia apicalis* as an optimal defense against sea star spongivory. *Marine Biology*, 143(3), 443-449. doi:10.1007/s00227-003-1109-5
- Gladkikh, A. S., Kalyuzhnaya, O. V., Belykh, O. I., Ahn, T. S., & Parfenova, V. V. (2014). Analysis of bacterial communities of two Lake Baikal endemic sponge species. *Microbiology*, 83(6), 787-797. doi:10.1134/s002626171406006x

- Golakoti, T., Yoshida, W. Y., Chaganty, S., & Moore, R. E. (2001). Isolation and structure determination of nostocyclopeptides A1 and A2 from the terrestrial Cyanobacterium *Nostoc* sp. ATCC53789. *Journal of Natural Products*, *64*(1), 54-59. doi:10.1021/np000316k
- Grachev, M., Zubkov, I., Tikhonova, I., Ivacheva, M., Kuzmin, A., Sukhanova, E., Sorokovikova, E., Fedorova, G., Galkin, A., Suslova, M., Netsvetayeva, O., Eletskaia, E., Pogadaeva, T., Smirnov, V., Ivanov, A., Shagun, V., Minaev, V., & Belykh, O. (2018). Extensive contamination of water with saxitoxin near the dam of the Irkutsk hydropower station reservoir (East Siberia, Russia). *Toxins*, *10*(10), 402. doi:10.3390/toxins10100402
- Haygood, M. G., Schmidt, E. W., Davidson, S. K., & Faulkner, D. J. (1999). Microbial symbionts of marine invertebrates: opportunities for microbial biotechnology. *Journal of Molecular Microbiology and Biotechnology*, *1*(1), 33-43.
- Hedges, J. I. (1992). Global biogeochemical cycles: Progress and problems. *Marine Chemistry*, *39*(1-3), 67-93. doi:10.1016/0304-4203(92)90096-s
- Hentschel, U., Fieseler, L., Wehrl, M., Gernert, C., Steinert, M., Hacker, J., & Horn, M. (2003). Microbial diversity of marine sponges. *Sponges (Porifera) Progress in Molecular and Subcellular Biology*, 59-88. doi:10.1007/978-3-642-55519-0_3
- Hentschel, U., Piel, J., Degnan, S. M., & Taylor, M. W. (2012). Genomic insights into the marine sponge microbiome. *Nature Reviews Microbiology*, *10*(9), 641-654. doi:10.1038/nrmicro2839
- Hoffmann, F., Radax, R., Woebken, D., Holtappels, M., Lavik, G., Rapp, H. T., Schläppli, M.-L., Schleper, C., & Kuypers, M. M. (2009). Complex nitrogen cycling in the sponge *Geodia barretti*. *Environmental Microbiology*, *11*(9), 2228-2243. doi:10.1111/j.1462-2920.2009.01944.x
- Hogg, M. M., Tendal, O. S., Conway, K. W., Pomponi, S. A., van Soest, R. W. M., Gutt, J., Krautter, M., & Roberts, J. M. (2010) Deep-sea sponge grounds: Reservoirs of biodiversity. *UNEP-WCMC Biodiversity Series No. 32*. UNEP-WCMC, Cambridge, UK.
- Holman, J. D., Tabb, D. L., & Mallick, P. (2014). Employing ProteoWizard to convert raw mass spectrometry data. *Current Protocols in Bioinformatics*, *46*(1). doi:10.1002/0471250953.bi1324s46
- Hörtensteiner, S., & Kräutler, B. (2011). Chlorophyll breakdown in higher plants. *Biochimica Et Biophysica Acta (BBA) - Bioenergetics*, *1807*(8), 977-988. doi:10.1016/j.bbabi.2010.12.007
- Imbs, A. B., & Latyshev, N. A. (1998). New Δ^5 and Δ^4 unsaturated medium- and long-chain fatty acids in the freshwater sponge *Baicalospongia bacilifera*. *Chemistry and Physics of Lipids*, *92*(2), 117-125. doi:10.1016/s0009-3084(98)00015-2
- Ishida, K., & Murakami, M. (2000). Kasumigamide, an antialgal peptide from the Cyanobacterium *Microcystis aeruginosa*. *The Journal of Organic Chemistry*, *65*(19), 5898-5900. doi:10.1021/jo991918f

- Itskovich, V. B., Kaluzhnaya, O. V., Veynberg, E., & Erpenbeck, D. (2015). Endemic Lake Baikal sponges from deep water. 1: Potential cryptic speciation and discovery of living species known only from fossils. *Zootaxa*, 3990(1), 123. doi:10.11646/zootaxa.3990.1.7
- Ivanisevic, J., Pérez, T., Ereskovsky, A. V., Barnathan, G., & Thomas, O. P. (2011). Lysophospholipids in the Mediterranean sponge *Oscarella tuberculata*: Seasonal variability and putative biological role. *Journal of Chemical Ecology*, 37(5), 537-545. doi:10.1007/s10886-011-9943-2
- Kaluzhnaya, O. V., Krivich, A. A., & Itskovich, V. B. (2012). Diversity of 16S rRNA genes in metagenomic community of the freshwater sponge *Lubomirskia baicalensis*. *Russian Journal of Genetics*, 48(8), 855-858. doi:10.1134/s1022795412070058
- Kaluzhnaya, O. V., & Itskovich, V. B. (2015). Bleaching of Baikalian sponge affects the taxonomic composition of symbiotic microorganisms. *Russian Journal of Genetics*, 51(11), 1153-1157. doi:10.1134/s1022795415110071
- Kampa, A., Gagunashvili, A. N., Gulder, T. A., Morinaka, B. I., Daolio, C., Godejohann, M., Miao, V. P. W., Piel, J., & Andresson, O. S. (2013). Metagenomic natural product discovery in lichen provides evidence for a family of biosynthetic pathways in diverse symbioses. *Proceedings of the National Academy of Sciences*, 110(33). doi:10.1073/pnas.1305867110
- Khanaev, I. V., Kravtsova, L. S., Maikova, O. O., Bukshuk, N. A., Sakirko, M. V., Kulakova, N. V., Butina, T. V., Nebesnykh, I. A., & Belikov, S. I. (2017). Current state of the sponge fauna (Porifera: Lubomirskiidae) of Lake Baikal: Sponge disease and the problem of conservation of diversity. *Journal of Great Lakes Research*, 44(1), 77-85. doi:10.1016/j.jglr.2017.10.004
- Kleinteich, J., Wood, S. A., Puddick, J., Schleheck, D., Küpper, F. C., & Dietrich, D. (2013). Potent toxins in Arctic environments – Presence of saxitoxins and an unusual microcystin variant in Arctic freshwater ecosystems. *Chemico-Biological Interactions*, 206(2), 423-431. doi:10.1016/j.cbi.2013.04.011
- Kulakova, N. V., Sakirko, M. V., Adelshin, R. V., Khanaev, I. V., Nebesnykh, I. A., & Pérez, T. (2018). Brown Rot Syndrome and changes in the bacterial community of the Baikal sponge *Lubomirskia baicalensis*. *Microbial Ecology*, 75(4), 1024-1034. doi:10.1007/s00248-017-1097-5
- Kurmayer, R., & Christiansen, G. (2009). The genetic basis of toxin production in cyanobacteria. *Freshwater Reviews*, 2(1), 31-50. doi:10.1608/frj-2.1.2
- Lagos, N., Onodera, H., Zagatto, P. A., Andrinolo, D., Azevedo, S. M. F. Q., & Oshima, Y. (1999). The first evidence of paralytic shellfish toxins in the freshwater cyanobacterium *Cylindrospermopsis raciborskii*, isolated from Brazil. *Toxicon*, 37(10), 1359-1373. doi:10.1016/s0041-0101(99)00080-x
- Laroche, M., Imperatore, C., Grozdanov, L., Costantino, V., Mangoni, A., Hentschel, U., & Fattorusso, E. (2007). Cellular localisation of secondary metabolites isolated from the Caribbean sponge *Plakortis simplex*. *Marine Biology*, 151(4), 1365-1373. doi:10.1007/s00227-006-0572-1

- Latyshev, N. A., Zhukova, N. V., Efremova, S. M., Imbs, A. B., & Glycina, O. I. (1992). Effect of habitat on participation of symbionts in formation of the fatty acid pool of fresh-water sponges of Lake Baikal. *Comparative Biochemistry and Physiology Part B: Comparative Biochemistry*, *102*(4), 961-965. doi:10.1016/0305-0491(92)90109-5
- Li, Z., Wang, Y., He, L., & Zheng, H. (2014). Metabolic profiles of prokaryotic and eukaryotic communities in deep-sea sponge *Neamphius huxleyi* indicated by metagenomics. *Scientific Reports*, *4*(1). doi:10.1038/srep03895
- Liu, H., Li, X., Lei, H., Zeng, G., Li, H., Liu, L., Xiao, R., Zhang, J., Sun, Z., Zhou, F., Zeng, Q., & Yang, L. (2019). Combined allelopathic effects of *Spirogyra* (Zygnematales: Zygnemataceae) and *Ceratophyllum demersum* (Ceratophyllales: Ceratophyllaceae) on the growth of *Microcystis aeruginosa* (Chroococcales: Microcystaceae). *Biologia*, *74*(8), 969-974. doi:10.2478/s11756-019-00238-7
- López-Legentil, S., Bontemps-Subielos, N., Turon, X., & Banaigs, B. (2006). Secondary metabolite and inorganic contents in *Cystodytes* sp. (Asciacea): Temporal patterns and association with reproduction and growth. *Marine Biology*, *151*(1), 293-299. doi:10.1007/s00227-006-0472-4
- López-Legentil, S., Erwin, P. M., Pawlik, J. R., & Song, B. (2010). Effects of sponge bleaching on ammonia-oxidizing archaea: Distribution and relative expression of ammonia monooxygenase genes associated with the barrel sponge *Xestospongia muta*. *Microbial Ecology*, *60*(3), 561-571. doi:10.1007/s00248-010-9662-1
- Macdonald, K. S., III, Rios, R., & Duffy, J. E. (2006). Biodiversity, host specificity, and dominance by eusocial species among sponge-dwelling alpheid shrimp on the Belize Barrier Reef. *Diversity and Distributions*, *12*(2), 165-178. doi:10.1111/j.1366-9516.2005.00213.x
- Mcmurray, S. E., Johnson, Z. I., Hunt, D. E., Pawlik, J. R., & Finelli, C. M. (2016). Selective feeding by the giant barrel sponge enhances foraging efficiency. *Limnology and Oceanography*, *61*(4), 1271-1286. doi:10.1002/lno.10287
- Mehner, C., Müller, D., Krick, A., Kehraus, S., Löser, R., Gütschow, M., Maier, A., Fiebig, H.-H., Brun, R., & König, G. M. (2008). A novel β -amino acid in cytotoxic peptides from the cyanobacterium *Tychonema* sp. *European Journal of Organic Chemistry*, *2008*(10), 1732-1739. doi:10.1002/ejoc.200701033
- Moore, M. V., Hampton, S. E., Izmet'eva, L. R., Silow, E. A., Peshkova, E. V., & Pavlov, B. K. (2009). Climate change and the World's "Sacred Sea"—Lake Baikal, Siberia. *BioScience*, *59*(5), 405-417. doi:10.1525/bio.2009.59.5.8
- Morrow, C., & Cárdenas, P. (2015). Proposal for a revised classification of the Demospongiae (Porifera). *Frontiers in Zoology*, *12*(1). doi:10.1186/s12983-015-0099-8
- Müller, W. E., Blumbach, B., & Müller, I. M. (1999). Evolution of the innate and adaptive immune systems. *Transplantation*, *68*(9), 1215-1227. doi:10.1097/00007890-199911150-00001

- Munoz, R., Teeling, H., Amann, R., & Rosselló-Móra, R. (2020). Ancestry and adaptive radiation of Bacteroidetes as assessed by comparative genomics. *Systematic and Applied Microbiology*, 43(2), 126065. doi:10.1016/j.syapm.2020.126065
- Murph, M., Tanaka, T., Pang, J., Felix, E., Liu, S., Trost, R., Godwin, A.K., Newman, R., & Mills, G. (2007). Liquid chromatography mass spectrometry for quantifying plasma lysophospholipids: Potential biomarkers for cancer diagnosis. *Methods in Enzymology Lipidomics and Bioactive Lipids: Specialized Analytical Methods and Lipids in Disease*, 1-25. doi:10.1016/s0076-6879(07)33001-2
- Negri, A. P., & Jones, G. J. (1995). Bioaccumulation of paralytic shellfish poisoning (PSP) toxins from the cyanobacterium *Anabaena circinalis* by the freshwater mussel *Alathyria condola*. *Toxicon*, 33(5), 667-678. doi:10.1016/0041-0101(94)00180-g
- Oksanen, J., Blanchet, F. G., Friendly, M., Kindt, R., Legendre, P., McGlinn, D., Minchin, P. R., O'Hara, R. B., Simpson, G. L., Solymos, P., Stevens, M. H. H., Szoecs, E., & Wagner, H. (2019). vegan: Community Ecology Package. R package version 2.5-6. <https://CRAN.R-project.org/package=vegan>
- Olson, J. B., Gochfeld, D. J., & Slattery, M. (2006). Aplysina red band syndrome: A new threat to Caribbean sponges. *Diseases of Aquatic Organisms*, 71, 163-168. doi:10.3354/dao071163
- Pile, A. J., Patterson, M. R., Savarese, M., Chernykh, V. I., & Fialkov, V. A. (1997). Trophic effects of sponge feeding within Lake Baikal's littoral zone. 2. Sponge abundance, diet, feeding efficiency, and carbon flux. *Limnology and Oceanography*, 42(1), 178-184. doi:10.4319/lo.1997.42.1.0178
- Pile, A. J., & Young, C. M. (2006). The natural diet of a hexactinellid sponge: Benthic–pelagic coupling in a deep-sea microbial food web. *Deep Sea Research Part I: Oceanographic Research Papers*, 53(7), 1148-1156. doi:10.1016/j.dsr.2006.03.008
- Pita, L., Rix, L., Slaby, B. M., Franke, A., & Hentschel, U. (2018). The sponge holobiont in a changing ocean: From microbes to ecosystems. *Microbiome*, 6(1). doi:10.1186/s40168-018-0428-1
- Pollock, F. J., Wada, N., Torda, G., Willis, B. L., & Bourne, D. G. (2016). White syndrome-affected corals have a distinct microbiome at disease lesion fronts. *Applied and Environmental Microbiology*, 83(2). doi:10.1128/aem.02799-16
- Pomati, F., Sacchi, S., Rossetti, C., Giovannardi, S., Onodera, H., Oshima, Y., & Neilan, B. A. (2000). The freshwater cyanobacterium *Planktothrix* sp. Fp1: Molecular identification and detection of paralytic shellfish poisoning toxins. *Journal of Phycology*, 36(3), 553-562. doi:10.1046/j.1529-8817.2000.99181.x
- Rasmussen, B., Fletcher, I. R., Brocks, J. J., & Kilburn, M. R. (2008). Reassessing the first appearance of eukaryotes and cyanobacteria. *Nature*, 455(7216), 1101-1104. doi:10.1038/nature07381
- R Core Team (2018). R: a language and environment for statistical computing. R Foundation for Statistical Computing, Vienna, Austria.

- Reiswig, H. M. (1971). Particle feeding in natural populations of three marine Demosponges. *The Biological Bulletin*, 141(3), 568-591. doi:10.2307/1540270
- Reiswig, H. M. (1975). Bacteria as food for temperate-water marine sponges. *Canadian Journal of Zoology*, 53(5), 582-589. doi:10.1139/z75-072
- Renard, E., Gazave, E., Fierro-Constain, L., Schenkelaars, Q., Ereskovsky, A., Vacelet, J., & Borchiellini, C. (2013). Porifera (Sponges): Recent knowledge and new perspectives. *eLS*. doi:10.1002/9780470015902.a0001582.pub2
- Reverter, M., Perez, T., Ereskovsky, A. V., & Banaigs, B. (2016). Secondary metabolome variability and inducible chemical defenses in the Mediterranean sponge *Aplysina cavernicola*. *Journal of Chemical Ecology*, 42(1), 60-70. doi:10.1007/s10886-015-0664-9
- Reverter, M., Tribalat, M., Pérez, T., & Thomas, O. P. (2018). Metabolome variability for two Mediterranean sponge species of the genus *Haliclona*: Specificity, time, and space. *Metabolomics*, 14(9). doi:10.1007/s11306-018-1401-5
- Rhoades, D. F. (1985). Offensive-defensive interactions between herbivores and plants: Their relevance in herbivore population dynamics and ecological theory. *The American Naturalist*, 125(2), 205-238. doi:10.1086/284338
- Rohde, S., & Schupp, P. J. (2011). Allocation of chemical and structural defenses in the sponge *Meloplhus sarasinorum*. *Journal of Experimental Marine Biology and Ecology*, 399(1), 76-83. doi:10.1016/j.jembe.2011.01.012
- Rützler, K. (1988). Mangrove sponge disease induced by cyanobacterial symbionts: Failure of a primitive immune system? *Diseases of Aquatic Organisms*, 5, 143-149. doi:10.3354/dao005143
- Salmaso, N., Cerasino, L., Boscaini, A., & Capelli, C. (2016). Planktic *Tychonema* (Cyanobacteria) in the large lakes south of the Alps: Phylogenetic assessment and toxigenic potential. *FEMS Microbiology Ecology*, 92(10). doi:10.1093/femsec/fiw155
- Schupp, P., Eder, C., Paul, V., & Proksch, P. (1999). Distribution of secondary metabolites in the sponge *Oceanapia* sp. and its ecological implications. *Marine Biology*, 135(4), 573-580. doi:10.1007/s002270050658
- Sebé-Pedrós, A., Degnan, B. M., & Ruiz-Trillo, I. (2017). The origin of Metazoa: A unicellular perspective. *Nature Reviews Genetics*, 18(8), 498-512. doi:10.1038/nrg.2017.21
- Shams, S., Capelli, C., Cerasino, L., Ballot, A., Dietrich, D., Sivonen, K., & Salmaso, N. (2015). Anatoxin-a producing *Tychonema* (Cyanobacteria) in European waterbodies. *Water Research*, 69, 68-79. doi:10.1016/j.watres.2014.11.006
- Simion, P., Philippe, H., Baurain, D., Jager, M., Richter, D. J., Franco, A. D., Roure, B., Satoh, N., Quéinnec, E., Ereskovsky, A., Lapébie, P., Corre, E., Delsuc, F., King, N., Wörheide, G., & Manuel, M. (2017). A large and consistent phylogenomic dataset supports sponges as the sister group to all other animals. *Current Biology*, 27(7), 958-967. doi:10.1016/j.cub.2017.02.031






- Sorokovikova, E. G., Belykh, O. I., Gladkikh, A. S., Kotsar, O. V., Tikhonova, I. V., Timoshkin, O. A., & Parfenova, V. V. (2013). Diversity of cyanobacterial species and phylotypes in biofilms from the littoral zone of Lake Baikal. *Journal of Microbiology*, *51*(6), 757-765. doi:10.1007/s12275-013-3240-4
- Sorokovikova, E., Belykh, O., Krasnopeev, A., Potapov, S., Tikhonova, I., Khanaev, I., Kabilov, M., Baturina, O., Podlesnaya, G., & Timoshkin, O. (2020). First data on cyanobacterial biodiversity in benthic biofilms during mass mortality of endemic sponges in Lake Baikal. *Journal of Great Lakes Research*, *46*(1), 75-84. doi:10.1016/j.jglr.2019.10.017
- Stal, L. J. (1995). Physiological ecology of cyanobacteria in microbial mats and other communities. *New Phytologist*, *131*(1), 1-32. doi:10.1111/j.1469-8137.1995.tb03051.x
- Sugiura, T., Fukuda, T., Miyamoto, T., & Waku, K. (1992). Distribution of alkyl and alkenyl ether-linked phospholipids and platelet-activating factor-like lipid in various species of invertebrates. *Biochimica Et Biophysica Acta (BBA) - Lipids and Lipid Metabolism*, *1126*(3), 298-308. doi:10.1016/0005-2760(92)90244-p
- Sweet, M., Burn, D., Croquer, A., & Leary, P. (2013). Characterisation of the bacterial and fungal communities associated with different lesion sizes of Dark Spot Syndrome occurring in the coral *Stephanocoenia intersepta*. *PLoS ONE*, *8*(4). doi:10.1371/journal.pone.0062580
- Sweet, M., Bulling, M., & Cerrano, C. (2015). A novel sponge disease caused by a consortium of micro-organisms. *Coral Reefs*, *34*(3), 871-883. doi:10.1007/s00338-015-1284-0
- Ternon, E., Perino, E., Manconi, R., Pronzato, R., & Thomas, O. P. (2017). How environmental factors affect the production of guanidine alkaloids by the Mediterranean sponge *Crambe crambe*. *Marine Drugs*, *15*(6), 181. doi:10.3390/md15060181
- Tidgewell, K., Clark, B. R., & Gerwick, W. H. (2010). The natural products chemistry of Cyanobacteria. In H.-W. Liu & L. Mander (Eds.), *Comprehensive Natural Products II: Chemistry and Biology* (pp. 141-188). Elsevier Science. doi:10.1016/b978-008045382-8.00041-1
- Timoshkin, O. A., Samsonov, D. P., Yamamuro, M., Moore, M. V., Belykh, O. I., Malnik, V. V., Sakirko, M. V., Shirokaya, A. A., Bondarenko, N. A., Domysheva, V. M., Fedorova, G. A., Kochetkov, A. I., Kuzmin, A. V., Lukhnev, A. G., Medvezhonkova, O. V., Nepokrytykh, A. V., Pasyukova, E. M., Poberezhnaya, A. E., Potapskaya, N. V., ... Bukshuk, N. A. (2016). Rapid ecological change in the coastal zone of Lake Baikal (East Siberia): Is the site of the world's greatest freshwater biodiversity in danger? *Journal of Great Lakes Research*, *42*(3), 487-497. doi:10.1016/j.jglr.2016.02.011
- Unson, M. D., & Faulkner, D. J. (1993). Cyanobacterial symbiont biosynthesis of chlorinated metabolites from *Dysidea herbacea* (Porifera). *Experientia*, *49*(4), 349-353. doi:10.1007/bf01923420
- Vacelet, J., & Donadey, C. (1977). Electron microscope study of the association between some sponges and bacteria. *Journal of Experimental Marine Biology and Ecology*, *30*(3), 301-314. doi:10.1016/0022-0981(77)90038-7

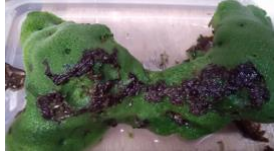




- Wang, M., Carver, J. J., Phelan, V. V., Sanchez, L. M., Garg, N., Peng, Y., . . . Bandeira, N. (2016). Sharing and community curation of mass spectrometry data with Global Natural Products Social Molecular Networking. *Nature Biotechnology*, *34*(8), 828-837. doi:10.1038/nbt.3597
- Waterbury, J. B. (2006). The cyanobacteria—isolation, purification and identification. In M. Dworkin, S. Falkow, E. Rosenberg, K.-H. Schleifer, & E. Stackebrandt (Eds.), *The Prokaryotes: Volume 4: Bacteria: Firmicutes, Cyanobacteria* (pp. 1053-1073). New York, NY: Springer US. doi:10.1007/0-387-30744-3_38
- Webster, N. S., Negri, A. P., Webb, R. I., & Hill, R. T. (2002). A spongin-boring a-proteobacterium is the etiological agent of disease in the Great Barrier Reef sponge *Rhopaloeides odorabile*. *Marine Ecology Progress Series*, *232*, 305-309. doi:10.3354/meps232305
- Webster, N. S. (2007). Sponge disease: A global threat? *Environmental Microbiology*, *9*(6), 1363-1375. doi:10.1111/j.1462-2920.2007.01303.x
- Weiner, D. R. (2002). *A little corner of freedom: Russian nature protection from Stalin to Gorbachev*. Berkeley, CA: University of California Press.
- Weisz, J. B., Lindquist, N., & Martens, C. S. (2008). Do associated microbial abundances impact marine demosponge pumping rates and tissue densities? *Oecologia*, *155*(2), 367-376. doi:10.1007/s00442-007-0910-0
- Wickham, H. (2016) *ggplot2: Elegant graphics for data analysis*. Springer-Verlag New York.
- Wilkinson, C. R., & Fay, P. (1979). Nitrogen fixation in coral reef sponges with symbiotic cyanobacteria. *Nature*, *279*(5713), 527-529. doi:10.1038/279527a0
- Wilkinson, C. R., Garrone, R., & Vacelet, J. (1984). Marine sponges discriminate between food bacteria and bacterial symbionts: Electron microscope radioautography and in situ evidence. *Proceedings of the Royal Society of London. Series B. Biological Sciences*, *220*(1221), 519-528. doi:10.1098/rspb.1984.0018
- Wolfender, J., Marti, G., & Queiroz, E. F. (2010). Advances in techniques for profiling crude extracts and for the rapid identification of natural products: Dereplication, quality control and metabolomics. *Current Organic Chemistry*, *14*(16), 1808-1832. doi:10.2174/138527210792927645


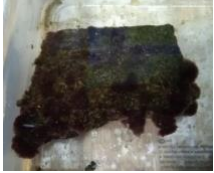

Appendix

Appendix 1

Table 4: Details about the specimens received for this study including specimen ID, sampling location, and observational and microscopy-aided descriptions of healthy and diseased sponges and biofilms. Images of most specimens in the lab, taken after collection and before lyophilization, are also included. The image for L_H1 was taken during collection and the image for R_U1 is not available.

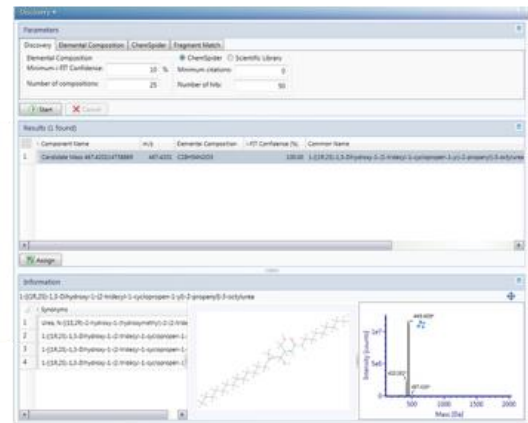
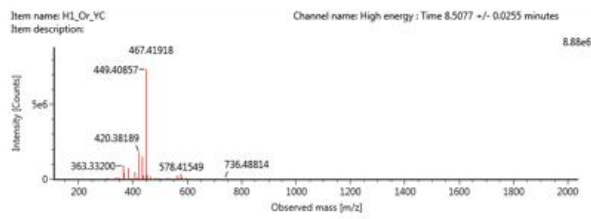
Specimen ID	Sampling Location	Description	Images
L_H1	Bolshie Koty	<i>Lubomirskia baikalensis</i> , healthy from background area without cyanobacteria	
L_H2	Bolshie Koty	L_H1 replicate	See L_H1
L_U1	Cape Tolsty	<i>Lubomirskia baikalensis</i> with bleaching and violet spots (<i>Pseudoanabaena</i> cyanobacteria, Diatom algae)	
L_U2	Bolshie Koty	<i>Lubomirskia baikalensis</i> with violet-brown spots	
L_U3	Bolshie Koty	<i>Lubomirskia baikalensis</i> (Diatom algae, cyanobacteria)	
B_H1	Bolshie Koty	<i>Baikalospongia</i> spp., healthy with some fungi	

B_U1	Cape Tolsty	<i>Baikalospongia</i> spp. with cyanobacterial spots	
B_U2	Cape Tolsty	Diseased <i>Baikalospongia</i> spp., tissue lesions with cyanobacteria	
B_U3	Cape Tolsty	Flat species of <i>Baikalospongia</i> , grew among cyanobacteria and diatom biofilms	
B_U4	Bolshie Koty	<i>Baikalospongia</i> spp. with violet cyanobacterial spots on body	
B_U5	Bolshie Koty	<i>Baikalospongia</i> spp. with violet spots and discolored body (fungi, bacteria)	
B_U6	Bolshie Koty	<i>Baikalospongia</i> spp. with massive cyanobacterial lesion (<i>Tychonema</i> , <i>Leptolyngbya</i>)	
B_U7	Bolshie Koty	<i>Baikalospongia</i> spp. with slight discolored zone (fungi, bacteria)	

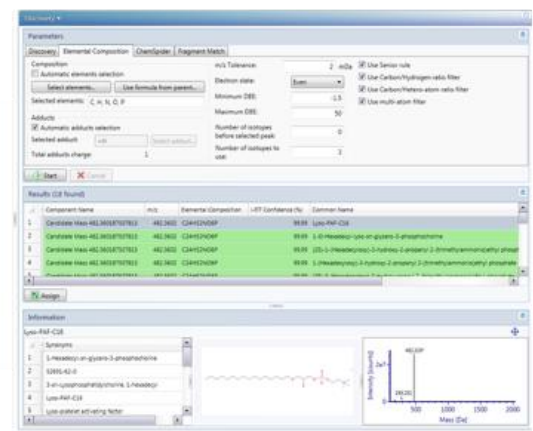
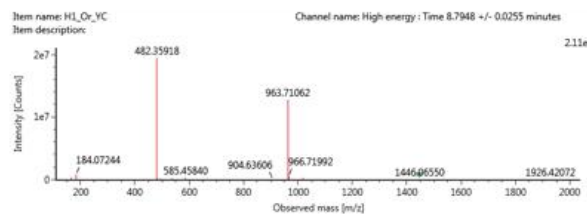
S_H1	Cape Tolsty	<i>Swartschewskia papyracea</i> with fungi? and bacteria	
S_U1	Cape Tolsty	<i>Swartschewskia papyracea</i> with bacterial biofilm	
R_H1	Cape Tolsty	<i>Rezenkovia ehinulata</i> , healthy	
R_U1	Cape Tolsty	<i>Rezenkovia ehinulata</i> with bacterial plaque	N/A
R_U2	Cape Tolsty	<i>Rezenkovia spp.</i> with brown spots (Diatom algae, <i>Synechococcus</i> / <i>Cyanobium</i> cyanobacteria)	
BF_1	Cape Tolsty	Biofilm with detritus from stone (Oscillatoriales cyanobacteria)	
BF_2	Cape Tolsty	Cyanobacterial biofilm from bottom stone next to <i>Baikalospongia spp.</i> (Dominated by <i>Tolypothrix distorta</i> (Nostocales))	
BF_3	Cape Tolsty	Cyanobacterial biofouling (Oscillatoriales)	

Appendix 2

a) m/z 467.4 RT 8.5 min



b) m/z 482.3 RT 8.7 min



c) m/z 524.3 RT 9.6/7 min

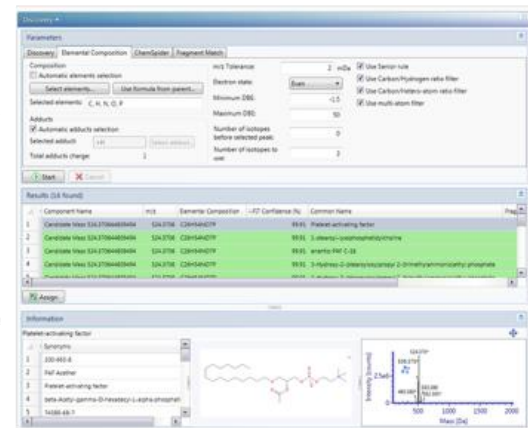
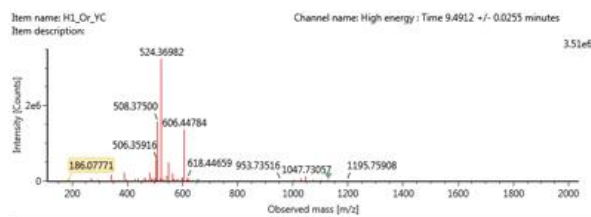
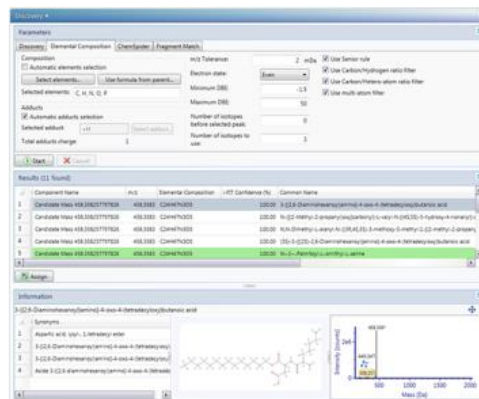
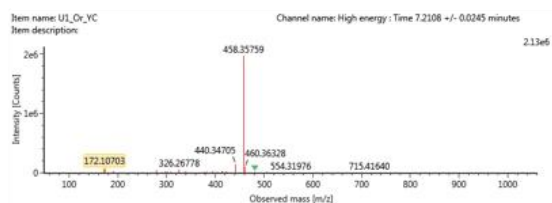
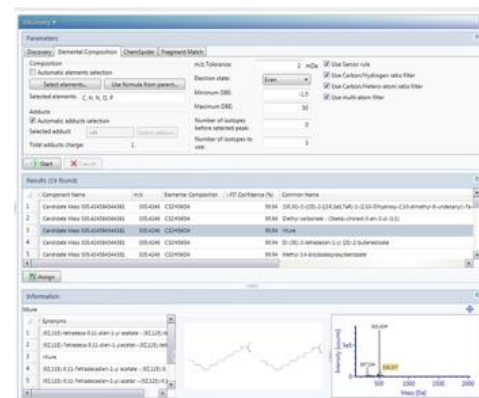
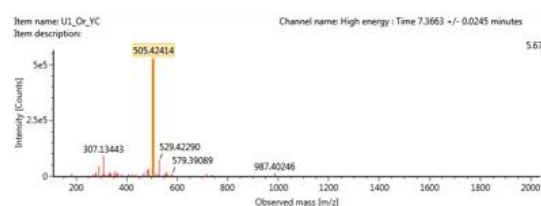


Figure 17: Examples of fragmentation patterns of molecules from Table 2 (Left) and a screenshot of the results of using the Discovery tool in UNIFI 1.9.4 software to elucidate the molecule's identity (Right).

a) m/z 458.3 RT 7.2 min



b) m/z 505.4 RT 7.3 min



c) m/z 533.2 RT 11.1 min

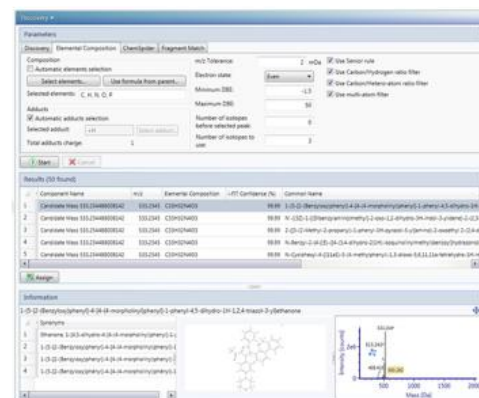
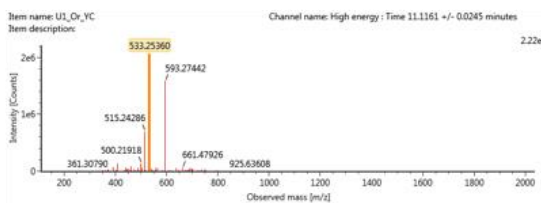


Figure 18: Examples of fragmentation patterns of molecules from Table 3 (Left) and a screenshot of the results of using the Discovery tool in UNIFI 1.9.4 software to elucidate the molecule's identity (Right).

Appendix 3

Compound_Name ^	ClusterIdx ^	View All Spectra ^	SharedPeaks	TIC Query ^	RT Query ^	MZErrorPPM	MassDiff ^	SpecMZ ^	LibMZ ^
<input type="text"/>	<input type="text"/>	<input type="text"/>	<input type="text"/>	<input type="text"/>	<input type="text"/>	<input type="text"/>	<input type="text"/>	<input type="text"/>	<input type="text"/>
PC(0:0/20:4); [M+H] ⁺ C28H51N107P1	2967	View Raw Spectra	6	2999.84	627.33	3454	1.88	541.46	543.33
PC(0:0/16:0); [M+H] ⁺ C24H51N107P1	1663	View Raw Spectra	6	28954.50	507.53	2624	1.30	496.63	495.33
Spectral Match to 1-Octadecanoyl-sn-glycero-3-phosphoethanolamine from NIST14	6874	View Raw Spectra	7	22985.10	526.72	566	0.55	964.18	963.63
PC(0:0/18:0); [M+H] ⁺ C26H55N107P1	2440	View Raw Spectra	8	65955.80	581.46	2577	1.35	524.71	523.36
PC(20:5/0:0); [M+H] ⁺ C28H49N107P1	2877	View Raw Spectra	6	2950.45	642.56	3578	1.94	539.38	541.32
PC(0:0/16:0); [M+H] ⁺ C24H51N107P1	1665	View Raw Spectra	6	2000.00	495.11	2240	1.11	496.44	495.33
PC(20:0/0:0); [M+H] ⁺ C28H59N107P1	3266	View Raw Spectra	6	3943.51	445.57	1826	1.01	552.40	551.39
PC(0:0/16:0); [M+H] ⁺ C24H51N107P1	1690	View Raw Spectra	6	2000.00	643.85	2226	1.10	496.44	495.33

Figure 19: Screenshot of a part of the identified compound list for *Lubomirskia* specimens (including L_H1, L_H2, L_U1, L_U2, L_U3) from molecular networking. Retrieved from Global Natural Products Social Molecular Networking (<https://gnps.ucsd.edu>).

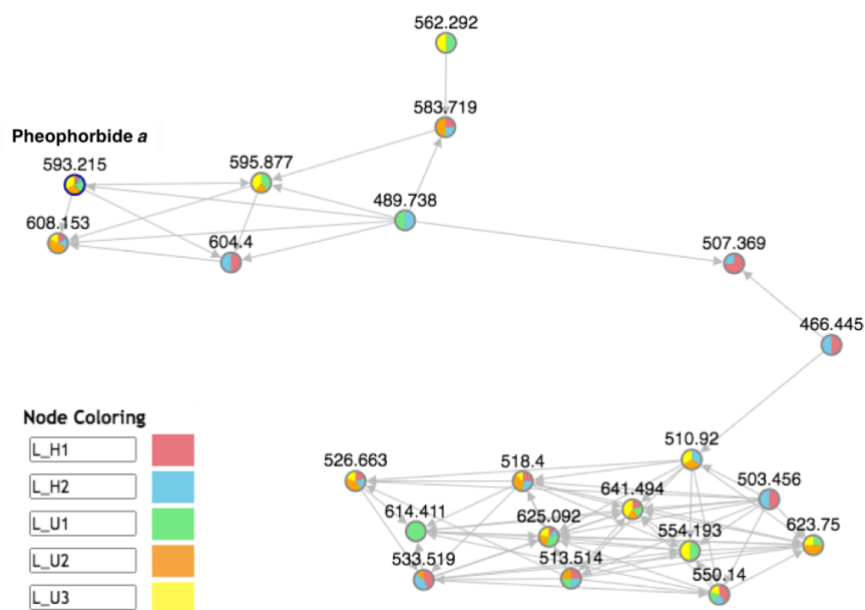


Figure 20: An example of how molecules cluster together to form families in molecular networking. This cluster contains molecules associated with pheophorbide a in *Lubomirskia* specimens (including L_H1, L_H2, L_U1, L_U2, L_U3). The colors of the nodes (circles) indicate the proportions of the numbers of spectra detected of each molecule in the different specimens. The m/z (H^+) of the molecules are listed next to each node and relationships between nodes and nodes groups are represented by the lines with arrows. Retrieved from Global Natural Products Social Molecular Networking (<https://gnps.ucsd.edu>).

Appendix 4

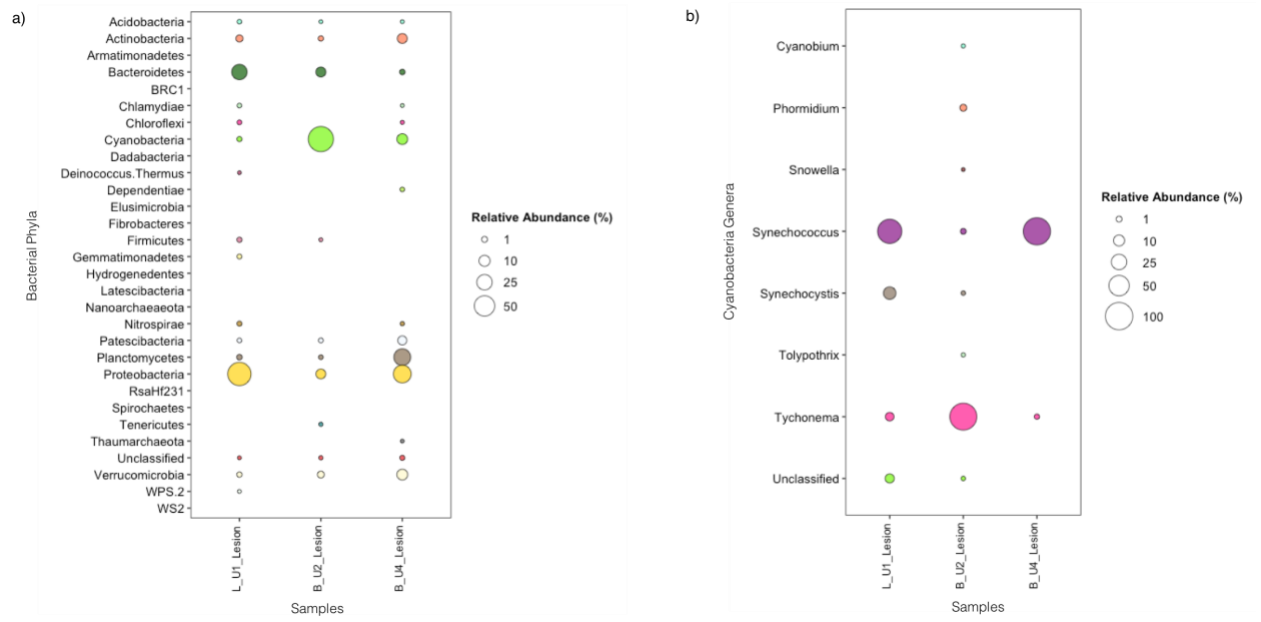


Figure 21: a) The relative abundances of the bacterial communities at phylum level in lesion sites from L_U1, B_U2, and B_U4. b) The relative abundances of the cyanobacteria genera in lesion sites from L_U1, B_U2, and B_U4.

